The LINNEAN SOCIETY of London BIOLOGICAL Journal of the Linnean Society

Biological Journal of the Linnean Society, 2016, **118**, 706–733. With 11 figures.

Microanatomical diversity of amniote ribs: an exploratory quantitative study

AURORE CANOVILLE[1]*, VIVIAN DE BUFFRÉNIL[2] and MICHEL LAURIN[2]

[1]*Bonn University, Steinmann Institute for Geology, Mineralogy and Paleontology, Nußallee 8, 53115, Bonn, Germany*
[2]*CR2P, Centre de Recherches sur la Paléobiodiversité et les Paléoenvironnements, Sorbonne Universités, CNRS/MNHN/UPMC, Muséum National d'Histoire Naturelle, Bâtiment de Géologie, Case postale 48, 43 rue Buffon, F-75231 Paris Cedex 05, Paris, France*

Received 23 November 2015; revised 14 December 2015; accepted for publication 14 December 2015

Bone microanatomical diversity in extant and extinct tetrapods has been studied extensively, using increasingly sophisticated quantitative methods to assess its ecological, biomechanical and phylogenetic significance. Most studies have been conducted on the appendicular skeleton, and a strong relationship was found between limb bone microanatomy and habitat preferences. Few comparative studies have focused on the microanatomy of the axial skeleton and its ecological signal. In the present study, we propose the first exploratory study of the microanatomical diversity of amniote ribs. Our comparative sample comprises 155 species of extant amniotes and encompasses the taxonomic, ecological, and body size diversity of this group. We standardized our sampling location to the midshaft of mid-dorsal ribs. Transverse sections were obtained from classical petrographic methods, as well as by X-ray microtomography. Most of the microanatomical and size characters of the ribs display a phylogenetic signal, which is an expected result and is also observed in amniote limb bones and vertebrae. We found a significant relationship between rib cortical thickness, global compactness, and lifestyle. As for the vertebrae, the development of the spongiosa in the medullary region appears to be strongly correlated with size. Even though an ecological signal was found in the inner structure of the ribs, additional work is needed to document the intra-individual variability of the rib microanatomy along the rib cage and within a single element. © 2016 The Linnean Society of London, *Biological Journal of the Linnean Society*, 2016, **118**, 706–733.

KEYWORDS: axial skeleton – virtual sections – comparative analysis – lifestyle adaptation – body size – bone microstructure – compactness.

INTRODUCTION

Over the past decade, bone microanatomical diversity (i.e. of the gross inner architecture of bones) in extant and extinct tetrapods has been studied extensively, sometimes using sophisticated quantitative methods to assess its ecological, biomechanical and phylogenetic significances (Laurin, Girondot & Loth, 2004; de Margerie *et al.*, 2005; Kriloff *et al.*, 2008; Canoville & Laurin, 2009, 2010; Dumont *et al.*, 2013; Quémeneur, de Buffrénil & Laurin, 2013; Houssaye, Tafforeau & Herrel, 2014). Bone microanatomy has been used to infer the habitat and locomotor mode of extinct taxa, along with gross morphology, taphonomy or stable isotope analyses (de Buffrénil *et al.*, 2010; Hayashi *et al.*, 2013; Amson *et al.*, 2014; Cooper *et al.*, 2014; Ibrahim *et al.*, 2014; Houssaye *et al.*, 2015a). Most studies have been conducted on the microanatomy of the appendicular skeleton, principally long limb bones (Wall, 1983; Currey & Alexander, 1985; Fish & Stein, 1991; Germain & Laurin, 2005; Kriloff *et al.*, 2008; Canoville & Laurin, 2009, 2010; Laurin, Canoville & Germain, 2011; Quémeneur *et al.*, 2013; Nakajima, Hirayama & Endo, 2014). Few studies have focused on the microanatomy of the axial skeleton (i.e. vertebrae and ribs) and its ecological signal (de Buffrénil *et al.*, 2010; Dumont *et al.*, 2013; Houssaye, 2013; Houssaye *et al.*, 2013, 2014; Waskow & Sander, 2014). The appendicular skeleton and the vertebral column

*Corresponding author. E-mail: canoville.aurore08@gmail.com

might be more greatly affected by locomotion and body support (and thus lifestyle adaptations) than the rib cage in tetrapods. Nonetheless, besides its role in ventilation, the rib cage is also affected by biomechanical constraints linked to locomotion and body support in general, especially in limbless tetrapods (Mosauer, 1932; Wake, 1979; Bramble & Carrier, 1983; Carrier, 1996; Clack, 2002; Fujiwara *et al.*, 2009).

Some studies have focused on the microanatomical diversity of vertebrae in extant mammals (Dumont *et al.*, 2013), extinct stegocephalians (Konietzko-Meier, Danto & Gądek, 2014), extant and extinct squamates (de Buffrénil & Rage, 1993; de Buffrénil *et al.*, 2008; Houssaye *et al.*, 2010, 2013; Houssaye & Bardet, 2012; Houssaye, 2013), and amniotes in general (Houssaye *et al.*, 2014). These works have revealed that body size is a major structural factor for vertebral microanatomy. Nonetheless, using large taxonomic samples (within Mammalia or Amniota), the various lifestyle and locomotor classes can be discriminated from vertebral microanatomy (Dumont *et al.*, 2013; Houssaye *et al.*, 2014). Even though fossorial taxa and shallow water dwellers generally show thicker vertebral cortices than pelagic and terrestrial animals, microanatomical differences mostly concern the organization and density of the trabecular networks (Dumont *et al.*, 2013; Houssaye *et al.*, 2014). Some taxa, such as extant snakes, do not show clear differences in vertebral microanatomy reflecting their lifestyle (de Buffrénil & Rage, 1993; Houssaye *et al.*, 2013). However, studies have shown that several extinct aquatic snakes exhibited pachyosteosclerotic vertebrae and ribs in the middle portion of the axial skeleton (de Buffrénil & Rage, 1993; Houssaye, 2013).

Vertebrae and ribs form a musculoskeletal unit because they are closely interconnected and prone to share some mechanical constraints, especially those provoked by axial muscle work. Indeed, their morphology and function evolved conjointly during the evolutionary history of tetrapods (Wake, 1979; Clack, 2002; Pierce *et al.*, 2013). Some studies have also highlighted that, for most aquatic taxa, whenever the vertebrae were pachyostotic or osteosclerotic, the associated ribs also presented bone mass increase (Houssaye, 2009, 2013). Moreover, amniotes exhibit variable rib morphologies, which are related to their lifestyle or locomotor adaptations. Birds, for example, exhibit distinct rib adaptations to diving, flying or terrestrial locomotion (Tickle *et al.*, 2007). Similarly, some fossorial or arboreal mammals apparently exhibit dorsoventrally expanded ribs, which increase the stability of the thorax during digging activity or arboreal locomotion (Jenkins, 1970; Wake, 1979). Comparable lifestyle-related differences at a microanatomical level can thus be expected in the ribs of tetrapods, even though differences in morphology are not necessarily linked to differences in bone microstructure (Meier *et al.*, 2013).

Taxonomically constrained studies, principally in mammals, have shown that rib compactness can be indicative of an aquatic lifestyle (de Buffrénil & Schoevaert, 1989; de Buffrénil *et al.*, 1990, 2010; Hayashi *et al.*, 2013). This relationship has been used to infer the ecology of extinct mammals and squamates (Houssaye & Bardet, 2012; Hayashi *et al.*, 2013; Houssaye, 2013; Amson *et al.*, 2014; Houssaye *et al.*, 2015a). However, no extensive interspecific comparative study has been conducted on the tetrapod microanatomy of the ribs with the aim of assessing the effects of habitat, body size, and phylogeny on the inner architecture of these bones. The necessity of such a quantitative study, conducted at a broad taxonomic scale, has been expressed repeatedly (Quémeneur *et al.*, 2013; Houssaye *et al.*, 2015a, b).

The study of ribs provides several practical advantages compared to limb long bones. (1) There are numerous elements per specimen and they are often preserved in the fossil record. Moreover, considering that ribs display few diagnostic characters, it is easier to obtain permission to sample them from museum curators and it is less invasive for the integrity of specimens. The great number of ribs in each individual also implies that they could contribute as much or even more than limb bones to body mass and density. Thus, they might contain a stronger ecological signal about habitat use than limb bones, whose signal might furthermore be blurred by biomechanical constraints linked with their weight-bearing role on land, a situation that should impact ribs to a lesser extent. (2) Such a study allows the sampling of almost all main amniote taxa, and could thus yield a broader understanding of microanatomical diversity in this group. Previous studies on long bones had to exclude limbless groups (such as most snakes, anguids, and amphisbeanians) from their analyses, as well as some aquatic taxa that lost their hindlimbs. (3) The study of rib inner architecture is complementary to previous works on long bones and vertebrae and further documents the general adaptation of the skeleton to environmental and biomechanical constraints.

We assume that ribs contribute significantly to the inertia and mass of the body in most tetrapods. We thus expect a decrease in rib compactness similar to that observed in limb long bones of flying taxa and pelagic deep divers, which require, respectively, to lower body mass or increase manoeuverability and swimming speed (Currey & Alexander, 1985; Webb & de Buffrénil, 1990; de Ricqlès & de Buffrénil,

2001). Conversely, we predict an increase in rib compactness in taxa living in coastal shallow water or swimming close to (or right below) the surface. An increase in bone mass (involving two distinct but sometimes coupled bone specializations called osteosclerosis and pachyostosis; de Ricqlès & de Buffrénil, 2001; de Buffrénil *et al.*, 2010), either localized or generalized in the skeleton, was observed in many aquatic tetrapods living in shallow water (Laurin *et al.*, 2004; Canoville & Laurin, 2009; Houssaye, 2009). Such heavy bones are assumed to serve as a ballast to counteract buoyancy in shallow water or to passively control the body trim (Domning & de Buffrénil, 1991; Taylor, 2000; de Ricqlès & de Buffrénil, 2001).

In the present study, we thus propose the first extensive investigation of rib microanatomical diversity in amniotes. The study aims to explore the broad interspecific diversity of amniote rib inner structure and to test quantitatively, and in a phylogenetic framework, its correlation with lifestyle and body size.

INSTITUTIONAL ABBREVIATIONS

AMNH, American Museum of Natural History, New York, NY, USA; p.c. VB, Personal collection of V. de Buffrénil; MHNL, musée des Confluences, centre de conservation et d'étude des collections, Lyon, France. MNHN, Muséum National d'Histoire Naturelle, Paris, France. ZFMK, Zoologisches Forschungsmuseum Alexander Koenig, Bonn, Germany.

MATERIAL AND METHODS

Biological sample

Our comparative sample comprises the ribs of 155 extant amniote species (60 lepidosaurs, 20 birds, two crocodilians, and 73 mammals) and 161 individuals and thus represents the largest sample used so far in such microanatomical studies (see Supporting information, Table S1). All bones were obtained from adults or subadults (judging from the size of the bones and the degree of epiphyseal fusion in associated long bones) and, according to museum records, most of them were from wild animals. The taxa were sampled to encompass the taxonomic, body size, and ecological diversity of amniotes (Fig. 1; see also Supporting information, Table S1). Our sample deliberately excludes turtles because their ribs are integrated into their carapace, which significantly modifies their architecture. This, and other peculiarities of the turtle body plan linked with the carapace (Lyson *et al.*, 2013), would bias comparisons with other taxa. Furthermore, changes in body density in turtles appear to have occurred largely through changes in the carapace and less in the rest of the skeleton (Scheyer & Sander, 2007; Kriloff *et al.*, 2008; Canoville & Laurin, 2010; Nakajima *et al.*, 2014). To investigate a possible influence of size on inner rib structure, we sampled different-sized animals for most amniote taxa, ranging from small squamates or rodents to large taxa such as the Komodo dragon, whales or ostriches (Fig. 1; see also Supporting information, Table S1). Recent studies on amniotes indeed show that body size explains a great percentage of the variance of vertebral inner architecture (Dumont *et al.*, 2013; Houssaye *et al.*, 2014), although this question has been less intensively investigated in long bones (Laurin *et al.*, 2004). In most cases, one specimen per species was sampled. When several specimens were collected for the same species, we used the species means in the statistical analyses.

Lifestyle categories

For every species, we coded the habitat using both primary literature and databases such as the Animal Diversity Web (Myers *et al.*, 2015) or the IUCN Red List of Threatened Species (IUCN, 2015).

Considering, on the one hand, the morphology, ethology, and ecology of the species sampled and, on the other hand, the hypothesis that ribs contribute significantly to the body inertia, we tentatively used the lifestyle categories listed below, mainly derived from Dumont *et al.* (2013) but adapted to the ecological diversity of amniotes. We initially recognized three categories for the limbless taxa (arboreal, terrestrial, and fossorial) distinct from the categories of limbed taxa because, unlike most other amniotes, their ribs are more directly involved in locomotion and could be affected differently by lifestyle.

State 0: Flying taxa
This category includes bats and some bird species. Birds that swim at the surface and that are occasional (unspecialized) divers (such as gulls or the mallard) were also assigned to this category.

State 1: Pelagic and active deep divers
This category includes some cetaceans and pinnipeds living in open waters and adapted to deep and prolonged dives for foraging.

State 2: Arboreal taxa (limbless taxa excluded)
This category includes some climbing and arboreal squamates, as well as some primates, mustelids, the red squirrel, and the two-toed sloth.

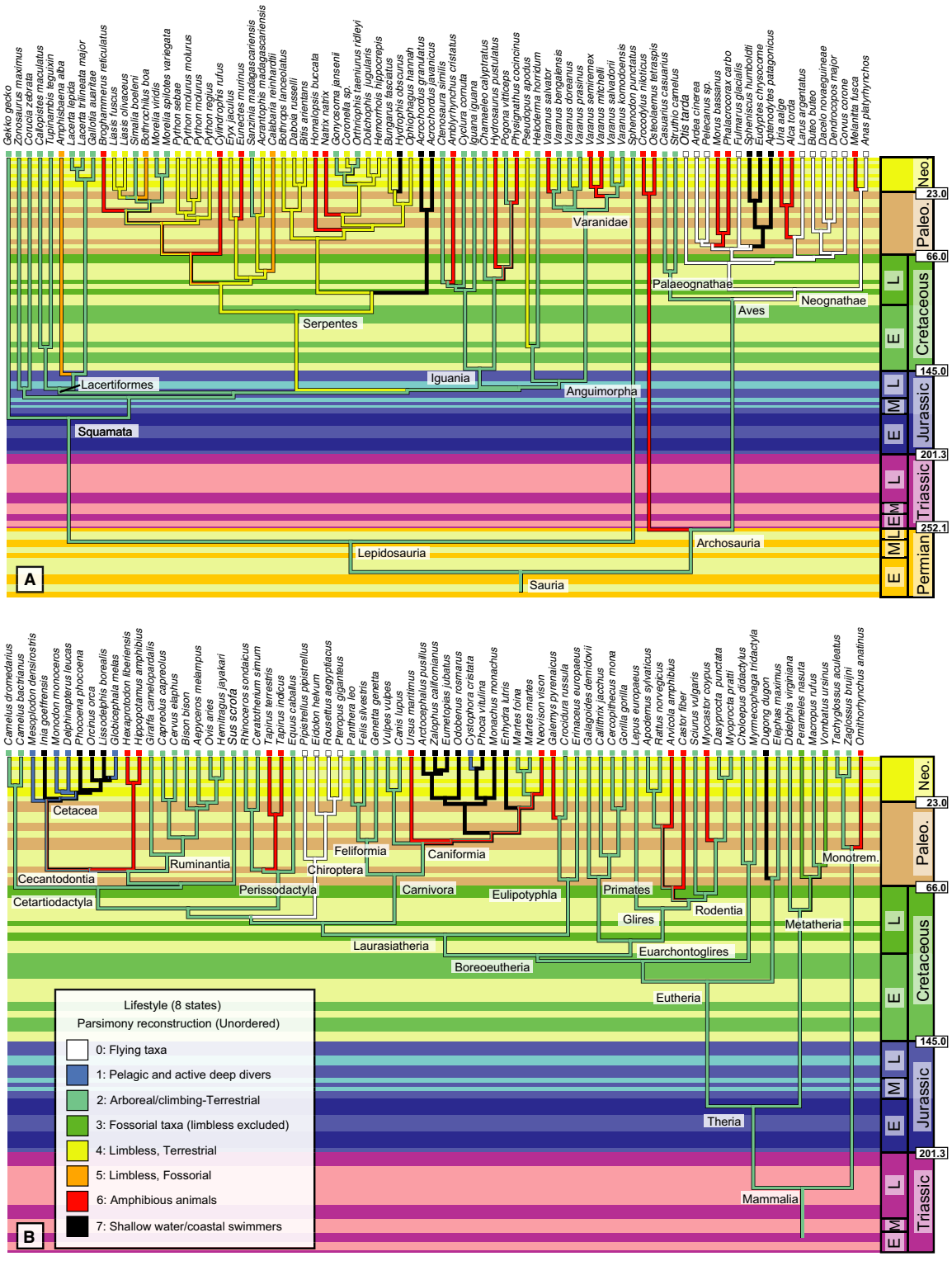

Figure 1. Reference phylogeny used in the present study for the phylogeny-informed analyses (A, diapsids; B, mammals). This time-calibrated supertree was compiled using the Stratigraphic Tools for MESQUITE (Josse, Moreau & Laurin, 2006) from previously published phylogenies (see Material and Methods). The divergence between diapsids and mammals was set approximately to 330 Myr, in the Carboniferous. The lifestyle (with eight character states, used in our statistical analyses) is optimized as an unordered character using parsimony. Neo., Neogene; Paleo., Paleogene; E, Early; M, Middle; L, Late.

State 3: Terrestrial (limbless taxa excluded)
This category encompasses various taxonomic groups (lepidosaurs, birds, mammals) that live on the ground.

State 4: Fossorial taxa (limbless taxa excluded)
This category includes two mammalian species that spend most of their time excavating burrows or digging in search for food: the common wombat and the long-nosed bandicoot.

State 5: Arboreal limbless taxa
This class consists of snakes that are good climbers or that spend a significant amount of time in trees (e.g. for foraging).

State 6: Terrestrial limbless taxa
This category encompasses mostly generalist species of snakes inhabiting various terrestrial environments. This class also includes the sheltopusik *Pseudopus apodus*, a limbless squamate.

State 7: Fossorial limbless taxa
This class comprises snakes that have been described as semi-fossorial of fossorial. This category also includes the red worm lizard *Amphisbaena alba*.

State 8: Amphibious taxa
This category comprises taxa living partly in fresh water or coastal environments and spending between 20% and 90% of their time in water. These taxa display no or only subtle morphological specializations to life in water. This includes not only both crocodilian species sampled, some mammals (e.g. the platypus, some mustelids, the polar bear, some rodents, both tapir and hippo species), but also some squamates such as the marine iguana *Amblyrhynchus cristatus* or some snakes that spend a significant amount of time in water such as the green anaconda *Eunectes murinus*. Finally, this group contains some flying birds that are also specialized divers, such as the Northern gannet *Morus bassanus* or the razorbill *Alca torda*.

State 9: Shallow water/coastal swimmers
This category integrates fully or mostly aquatic coastal or fresh water dwellers. This mostly includes taxa with clear morphological specializations to the aquatic environment, such as flightless diving birds (penguins), the dugong, and most pinnipeds. We also decided to assign to this class some cetaceans spending most of their time swimming close to the surface or in shallow coastal or riverine environments (e.g. the Amazon river dolphin *Inia geoffrensis*). Finally, this category also contains three aquatic snakes living in brackish or marine environments. Note that this category includes both active swimmers, such as pinnipeds and the flightless diving birds, and much more sluggish ones, such as the dugong, because we consider that the shallow depth at which these taxa swim imposes more severe constraints than inertia of the skeleton in the most active swimmers. Of course, it would also have been defensible to divide this category into two if we had had a greater sample size.

This ordering reflects our a priori ideas about how lifestyle should be related to rib overall compactness, rather than the way lifestyle may have evolved. In the list above, states are listed from those assumed to have the lightest ribs to those in which we expect the greatest rib density. However, we also expected that our coding might be too fine given our limited sample, and the order between some states was difficult to determine a priori. This problem could have resulted in a loss of power because our analytical methods (see below) assume that states are ordered linearly, and setting two states into the wrong order should reduce power more than combining these two states. We thus performed exploratory analyses to obtain the best compromise between sample size and information contained within the states, as assessed by the strength of the relationship detected between lifestyle and bone microanatomy. In the analyses of the ecological signal, this led us to combine the terrestrial (state 3) and limbless arboreal (state 5) categories with state 2 (initially containing only arboreal taxa, excluding limbless forms). Our final coding thus retains eight states, rather than ten [state 0: flying taxa; state 1: pelagic and active deep divers; state 2: arboreal/climbing taxa (including limbless) and terrestrial; state 3: fossorial taxa (limbless taxa excluded); state 4: limbless, terrestrial; state 5: limbless, fossorial; state 6: amphibious taxa; state 7: shallow water/coastal swimmers]. We found that a further lowering of the number of states reduced the power to identify relationships between bone microanatomy and lifestyle; thus, in contrast to our previous studies, we did not use a binary or ternary coding of lifestyle. To prevent our ordering selection protocol from introducing a bias into the analyses, we performed corrections for multiple tests using the false discovery rate (Benjamini & Hochberg, 1995; Curran-Everett, 2000) on all our tests, even though we report only the results with the optimal coding of lifestyle.

Sampling strategy

Considering the high degree of interspecific and intraspecific variability in the number, morphology, and probably the microstructure of the ribs, we attempted to standardize our sampling location as

much as possible to reduce any discrepancy or inconsistency between samples.

Indeed, the relative form (length, thickness, and curvature) and number, and, when present, the pattern of regional variation within the rib series (e.g. cervical, thoracic, lumbar, sacral, caudal ribs) are all diverse at both broad and fine taxonomic scales within tetrapods (Clack, 2002; Asher *et al.*, 2011; Casha *et al.*, 2015a). We did not sample gastralia because their ontogenetic origin (as dermal elements) differs from that of true ribs (dorsal, endoskeletal elements); therefore, we standardized our sample by sectioning only dorsal and thoracic ribs (when this regional differentiation exists).

Within the rib series, the various elements usually show differences in morphologies and microstructures that may reflect their mechanical loads (Fujiwara *et al.*, 2009; Waskow & Sander, 2014; Casha *et al.*, 2015a, b). However, identifying the rib most affected by the mechanical load and the lifestyle is difficult because it depends on diverse factors such as locomotion mode and posture, and the identity of the optimal rib (for our purpose) may thus be variable between taxa (Bramble & Carrier, 1983; Fujiwara *et al.*, 2009). Unfortunately, most of the literature related to intraspecific variability in rib architecture is medically-driven and pertains to humans; it emphasizes assessments of the impact of ageing or traumatic events on the rib cage biomechanics (Yoganandan & Pintar, 1998; Li *et al.*, 2010; Mitton *et al.*, 2014; Casha *et al.*, 2015a,b) or the effect of nutritional or physiological stresses (Heinrich, 2015).

Thus, for each limbed species, only the mid-thoracic rib was selected. This usually corresponds to one of the longest ribs in the thoracic rib series. For limbless species, we also sampled one rib among the largest ones along the vertebral column.

Finally, it has also been observed for some tetrapod species that rib compactness varies in a single element between the proximal head and the distal end (Waskow & Sander, 2014; D'Emic, Smith & Ansley, 2015; Houssaye *et al.*, 2015a). Nonetheless, Waskow & Sander (2014) noted that rib compactness is most uniform along the rib shaft for sauropod dinosaurs. This was also observed from computed tomography (CT) scans for the various amniote species sampled in the present study (A. Canoville, personal observations). We thus restricted our preliminary study to the mid-shaft of the sampled rib (Fig. 2B).

Technical processing of the ribs

Each rib was photographed and measured in accordance with the protocol proposed by de Buffrénil *et al.*, 2010 (Fig. 2A) to document rib length, which

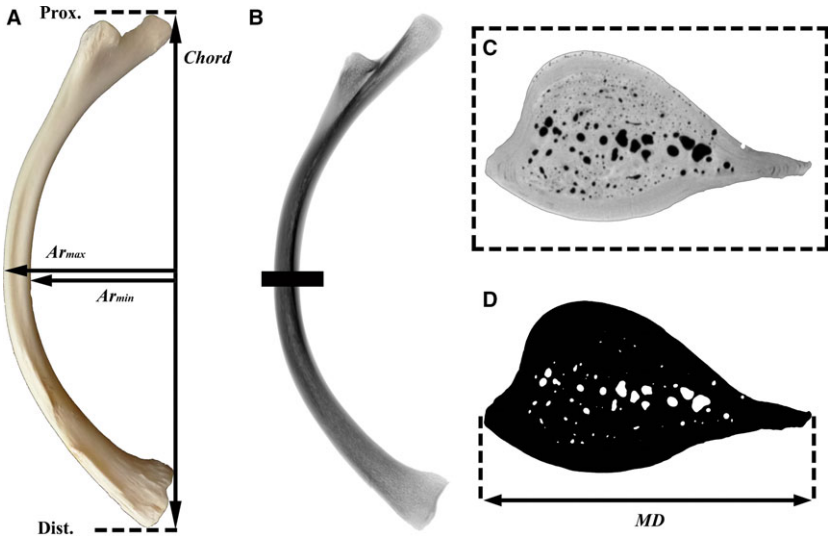

Figure 2. Technical processing of the ribs and cross-sections. A, median ribs were measured before being sectioned or scanned via computed tomography (CT), as shown on the rib of *Crocodylus niloticus* ZFMK 5249. The mean arrow, Ar_{mean} (not shown), corresponds to 0.5 (Ar_{min} + Ar_{max}); rib length (*LG*) is: *Chord* + Ar_{mean}. B, some ribs were CT scanned to produce virtual sections. Each rib was sampled at mid-length. The black rectangle marks the level of the rib where the cross-section has been sampled for analysis. C, virtual cross-section extracted from the shaft of the rib. D, each cross-section was converted into a binary image using PHOTOSHOP CS6 (Adobe Systems Inc.) for analysis in BONE PROFILER (Girondot & Laurin, 2003) and IMAGEJ (Abramoff *et al.*, 2004). On such images, the osseous tissue appears black and the cavities (medullary cavity, resorption lacunae, and vascular canals) are white. Ar_{min}, small arrow at maximum bend; Ar_{max}, large arrow at maximum bend; Dist., distal; *MD*, maximal diameter of the cross-section; Prox., proximal.

is one of the parameters used as a proxy for body size.

The sections were obtained either through classical sectioning methods, or through X-ray microtomography (CT scans; Fig. 2C; see also Supporting information, Table S1). The conventional ground sections obtained from the initial bone samples were 100 ± 10 μm thick. They were realized at the Muséum National d'Histoire Naturelle, Paris, France using the conventional methods employed for this kind of preparation (Lamm, 2013).

Some bones were scanned at the Steinmann Institute (Bonn, Germany) using a Geophoenix X-ray generator. The reconstructions were performed with DATOX/RES and the virtual sections were obtained in VG STUDIO MAX, version 2.0 (Volume Graphics).

Images of all cross-sections, real or virtual, were then converted into binary images (Fig. 2D) and analyzed with BONE PROFILER (Girondot & Laurin, 2003) and IMAGEJ (Abramoff, Magalhães & Ram, 2004) to extract morphometric and quantitative microanatomical parameters that describe bone inner architecture (see Supporting information, Table S1).

Quantitative parameters

Size descriptors

Three continuous variables express the length of the ribs and bulk of each bone at the sampling location. (1) Rib length (*LG*, in mm) was calculated as the sum of the rib *chord* and the mean rib arrow, or Ar_{mean} (*sensu* de Buffrénil *et al.*, 2010). The mean rib arrow refers to the mean of the lengths of two vectors (Ar_{min} and Ar_{max}) projected perpendicularly from the *chord* to the inner and outer rib surfaces, respectively, at maximum rib bend (Fig. 2A); this measurement was added to the rib *chord* to take into account the curvature of the rib shaft. (2) The maximal diameter (in mm) and (3) the total sectional area (expressed in mm^2 and including actual bone tissue and all inner cavities) of the cross-section. These were measured in IMAGEJ. We took into account the parameter *MD* because it has been repeatedly used in similar studies as a proxy of body size (Canoville & Laurin, 2009, 2010; Quémeneur *et al.*, 2013; Houssaye *et al.*, 2015b). However, we are aware that this parameter is not as representative of rib bulk as the total cross-sectional *Area* because, for the same given *MD*, a rib could be either flat or almost circular in cross-section. Our analyses should show to what extent *MD* is an acceptable substitute of the cross-section *Area* in this context. These three parameters (*LG*, *MD*, and *Area*) were used in statistical analyses as proxies of body size.

Compactness profile parameters

Four main compactness profile parameters (*S*, *P*, *Min* and *Max*) describing the organization of the bone tissue along the radius of the cross-section were obtained in BONE PROFILER (Girondot & Laurin, 2003), a computer program widely used in microanatomical studies (Canoville & Laurin, 2010; Meier *et al.*, 2013; Quémeneur *et al.*, 2013; Houssaye *et al.*, 2015b).

(1) Parameter *S* reflects the relative width of the transition zone between the medullary and the cortical regions. *S* tends towards 0 when the transition between the medullary cavity and the compact cortex is abrupt and a perimedullary spongiosa is absent.
(2) Parameter *P* materializes the position of the transition zone between the medullary and the cortical regions and is thus proportional to the size of the medullary cavity.
(3) Parameter *Min* represents the compactness in the centre of the section. A value > 0 usually indi-

Figure 3. Mid-shaft cross-sections of the median ribs of various lepidosaurs (A, Sphenodontia; B-b, Squamata), excluding snakes. The various lifestyles and locomotor patterns are given in brackets. The sections sharing the same scale bar are sometimes delimited by a grey rectangle for clarity. A, *Sphenodon punctatus* ZFMK 70219 (terrestrial); B, *Ctenosaura similis* ZFMK 14845 (terrestrial); C, *Amblyrhynchus cristatus* ZFMK 94250 (amphibious); D, *Iguana iguana* ZFMK 70426 (arboreal); E, *Cyclura cornuta* ZFMK 14843 (terrestrial); F, *Varanus komodoensis* ZFMK 64698 (terrestrial); G, *Varanus bengalensis nebulosus* ZFMK 59018 (terrestrial); H, *Varanus salvator* ZFMK 90471 (amphibious); I, *Varanus salvadorii* ZFMK 90997 (arboreal); J, *Varanus doreanus* ZFMK 92174 (terrestrial); K, *Varanus mitchelli* ZFMK 54250 (amphibious); L, *Varanus semiremex* ZFMK 54247 (amphibious); M, *Varanus prasinus* ZFMK 5234 (arboreal); N, *Pseudopus apodus* ZFMK 7840 (limbless, terrestrial); O, *Heloderma horridum* ZFMK 14834 (terrestrial); P, *Pseudopus apodus* MHNL 50.00.1248 (limbless, terrestrial); Q, *Corucia zebrata* ZFMK 5226 (arboreal); R, *Amphisbaena alba* MHNL 50.00.1247 (limbless, fossorial); S, *Salvator merianae* ZFMK 53532 (terrestrial); T, *Callopistes maculatus* ZFMK 7853 (terrestrial); U, *Gecko gecko* ZFMK 5123 (arboreal); V, *Timon lepidus* ZFMK 76997 (terrestrial); W, *Lacerta trilineata major* ZFMK 3509 (terrestrial); X, *Gallotia auaritae* ZFMK 96468 (terrestrial); Y, *Hydrosaurus pustulatus* ZFMK 9981 (amphibious); Z, *Physignathus cocincinus* ZFMK 9995 (arboreal, amphibious); a, *Pogona vitticeps* ZFMK 54246 (terrestrial, climbing); b, *Zonosaurus maximus* ZFMK 7825 (terrestrial).

cates the presence of trabeculae in the centre of the section.

(4) Parameter *Max* corresponds to the compactness in the outermost cortex.

The radial versions of these parameters (S_{rad}, P_{rad}, Min_{rad}, and Max_{rad}) were also compiled from BONE PROFILER. Further details on how these parameters are calculated are provided in Girondot &

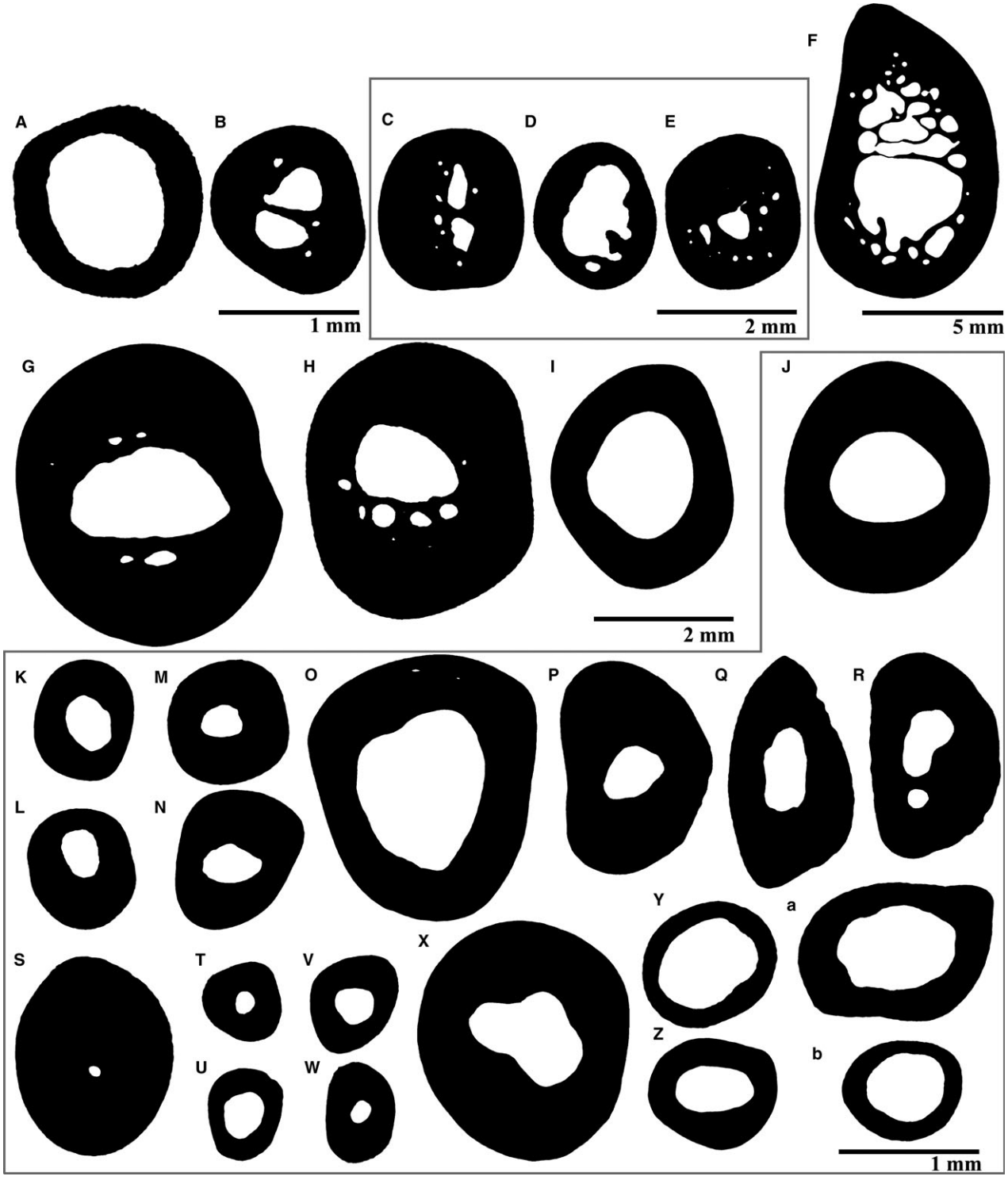

Figure 4. Mid-shaft cross-sections of the median ribs of various snake species. The various lifestyles and locomotor patterns are given in brackets. The sections sharing the same scale bar are sometimes delimited by a grey rectangle for clarity. A, *Eunectes murinus* MNHN. AC 1940-353 (amphibious); B, *Eunectes murinus* ZFMK 5179 (amphibious); C, *Acrantophis madagascariensis* ZFMK 86469 (terrestrial); D, *Sanzinia madagascariensis* ZFMK 70428 (arboreal); E, *Calabaria reinhardtii* ZFMK 89190 (terrestrial, fossorial); F, *Eryx jaculus* MNHN. AC 1889-409 (terrestrial); G, *Broghammerus reticulatus* MNHN. AC 1931-70 (amphibious); H, *Python sebae* ZFMK 54623 (terrestrial); I, *Python molurus* ZFMK 81775 (terrestrial); J, *Python sebae* ZFMK 5199 (terrestrial); K, *Python regius* ZFMK 92527 (terrestrial); L, *Bungarus fasciatus* ZFMK 61719 (terrestrial); M, *Bothrochilus boa* ZFMK 5203 (terrestrial, fossorial); N, *Morelia spilotes variegata* ZFMK 84282 (arboreal); O, *Morelia boeleni* ZFMK 76305 (terrestrial, arboreal); P, *Python molurus molurus* ZFMK 83431 (terrestrial); Q, *Liasis fuscus* ZFMK 54624 (terrestrial); R, *Liasis olivaceus* ZFMK 74535 (terrestrial); S, *Orthriophis taeniurus (Elaphe taeniura) ridleyi* ZFMK 5215 (terrestrial; arboreal); T, *Bitis arientans* MNHN. AC 1885-246 (terrestrial); U, *Bitis arientans* ZFMK 5210 (terrestrial); V, *Dolichophis jugularis* MHNL 50.00.1262 (terrestrial); W, *Daboia russelli* ZFMK 61721 (terrestrial); X, *Bothrops lanceolatus* MNHN. AC 1887-934 (terrestrial); Y, *Acrochordus javanicus* MNHN. AC 1869-783 (aquatic); Z, *Gonyosoma jansenii* ZFMK 76709 (arboreal); a, *Coronella* sp. MHNL 50.00.1261 (terrestrial); b, *Ophiophagus hannah* MNHN. AC 2002-42 (terrestrial); c, *Hemorrhois hippocrepis* ZFMK 5204 (terrestrial); d, *Morelia viridis* ZFMK 5211 (arboreal); e, *Hydrophis obscurus* MHNL 50.00.1243 (aquatic); f, *Natrix natrix* MNHN. AC 1874-535 (amphibious); g, *Cylindrophis rufus* MHNL 50.00.1246 (amphibious); h, *Natrix natrix* MHNL 50.00.1259 (amphibious); i, *Homalopsis buccata* MHNL 50.00.1265 (amphibious); j, *Acrochordus granulatus* MHNL 50.00.1240 (aquatic).

Laurin (2003) and Laurin *et al.* (2004). Finally, the global compactness (*Comp.*) of the cross-section (an index varying from 0 to 1 and representing the actual area occupied by mineralized bone tissue, expressed as a proportion of the total sectional area) was also obtained from BONE PROFILER.

Statistical analysis

Reference phylogeny

Most statistical analyses reported below require a reference phylogeny. We thus used an updated version (with newly added terminal taxa) (Fig. 1) of our previously published supertree (Canoville & Laurin, 2010; Quémeneur *et al.*, 2013). To update the time-calibrated phylogeny of birds, we referred to Jarvis *et al.* (2014). The divergence date between *Crocodylus* and *Osteolaemus* is in accordance with Oaks (2011). For squamates, global typology and divergence times were obtained from Hedges & Vidal (2009), Wiens *et al.* (2012), Pyron, Burbrink & Wiens (2013), and Wiens & Lambert (2014). The topology of Iguania is in accordance with Townsend *et al.* (2011) and Blankers *et al.* (2013), and for that of varanids is from Conrad *et al.* (2011). The topology and divergence dates of snake phylogeny are in accordance with Vidal *et al.* (2009), Pyron *et al.* (2013), and Reynolds, Niemiller & Revell (2014). Mammalian phylogeny is in accordance with Meredith *et al.* (2011) whenever it provided sufficient resolution. However, given that the study by Meredith *et al.* (2011) included only terminal taxa typically ranked as families, whenever at least two terminals were included within a nominal family, we had to obtain divergence times from other sources, typically from TIMETREE2 (Kumar & Hedges, 2011). Topological information was also obtained from other sources whenever at least three terminals were included within a nominal family. We used Galewski *et al.* (2006) for Muridae, Yonezawa *et al.* (2007) for Mustelidae, Agnarsson, Kuntner & May-Collado (2010) for Otariidae, Agnarsson *et al.* (2011) and Teeling (2009) for chiropterans, Bibi (2013) for Hassanin *et al.* (2012) for Delphinidae.

Phylogenetic signal

We assessed the presence of a phylogenetic signal, partly because of the inherent interest in this question but, more importantly, to determine whether phylogeny-informed analytical methods had to be used. For this, we used the method described in Laurin (2004), which consists of comparing the amount of character change implied by the reference tree with that of a population of randomized trees. For continuous characters, squared length (Maddison, 1991) is used, which requires keeping the same tree length distribution. Hence, we randomly reshuffled the values of the terminal taxa over the tree. For discrete characters, other randomization procedures could be employed, although, for simplicity's sake, we used the same. We produced 10 000 random trees. This test was performed in MESQUITE, version 3.0 (Maddison & Maddison, 2014).

Ecological signal

The presence of an ecological signal (i.e. a quantifiable relationship between lifestyle and rib microanatomy or size) was tested using two methods: pairwise comparisons (Maddison, 2000) and, subsequently, a sign test on phylogenetic independent contrasts (FIC) (Felsenstein, 1985). The second method is implemented in the PDAP: PDTREE module (Midford, Garland & Maddison, 2010) for MESQUITE. Pairwise comparisons, which are implemented in the stock ver-

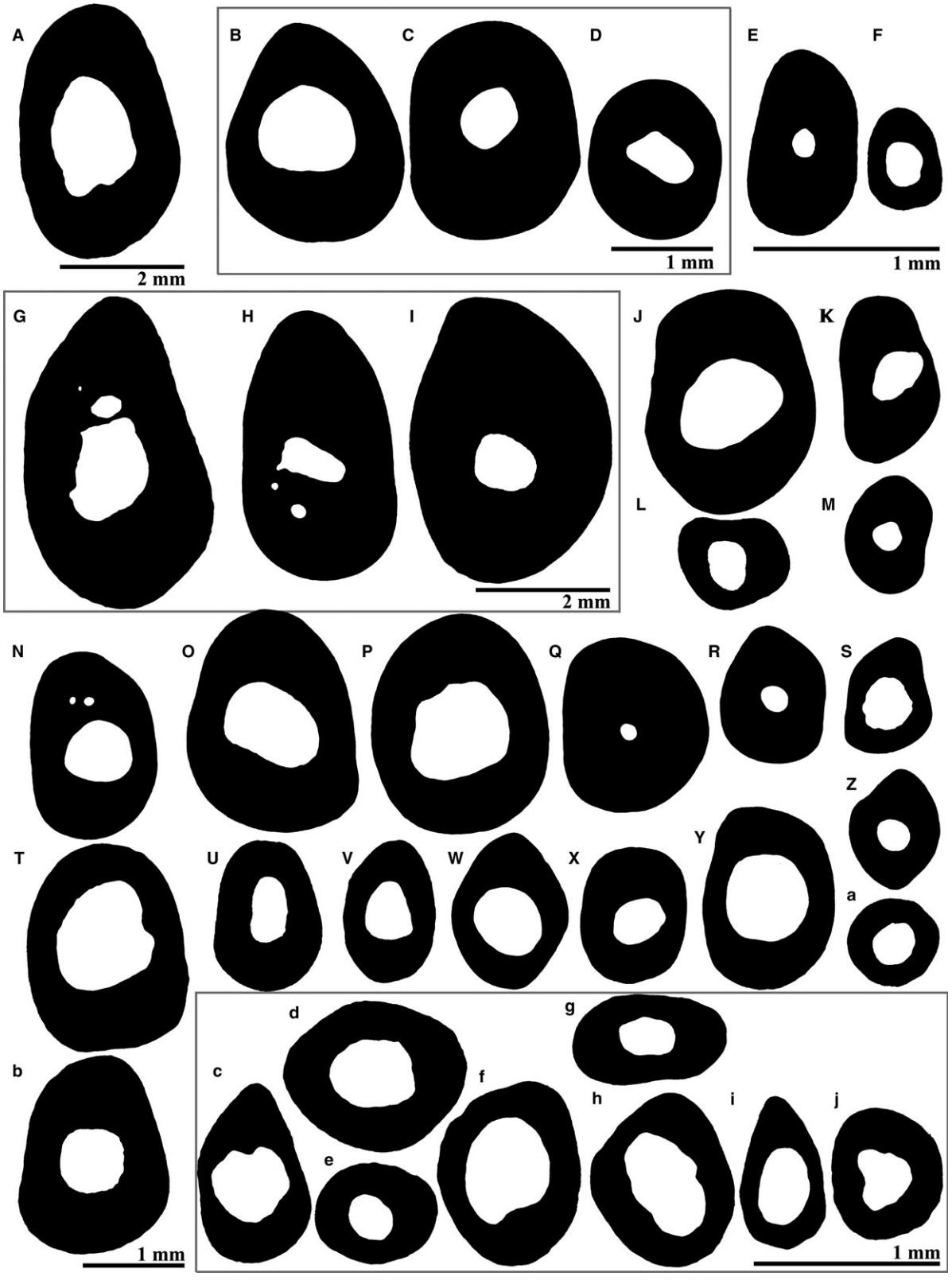
A
B
C
D
E
F
2 mm
1 mm
1 mm
G
H
I
J
K
L
M
2 mm
N
O
P
Q
R
S
Z
T
U
V
W
X
Y
a
b
c
d
e
f
g
h
i
j
1 mm
1 mm

Figure 5. Mid-shaft cross-sections of the median ribs of various archosaurs (A, B, crocodilians; C–V, birds). The various lifestyles and locomotor patterns are given in brackets. The sections sharing the same scale bar are sometimes delimited by a grey rectangle for clarity. A, *Crocodylus niloticus* ZFMK 5249 (amphibious); B, *Osteolaemus tetraspis* ZFMK 93026 (amphibious); C, *Casuarius casuarius* ZFMK 79sk5 (flightless, terrestrial); D, *Struthio camelus* ZFMK 83sk13 (flightless, terrestrial); E, *Otis tarda* ZFMK 78sk11 (flying); F, *Pelecanus* sp. ZFMK 78sk63 (flying, surface swimmer); G, *Anas platyrhynchos* ZFMK 60503 (flying, surface swimmer); H, *Morus bassanus* ZFMK 74sk1 (amphibious: flying, diving); I, *Phalacrocorax carbo* ZFMK 86sk178 (amphibious: flying, diving); J, *Melanitta nigra* ZFMK 75sk68 (amphibious: flying, diving); K, *Aptenodytes patagonicus* ZFMK 011sk18 (aquatic: flightless, diving); L, *Eudyptes chrysocome* ZFMK 75sk64 (aquatic: flightless, diving); M, *Spheniscus humboldti* ZFMK 74sk12 (aquatic: flightless, diving); N, *Buteo buteo* ZFMK 78sk187 (flying); O, *Ardea cinerea* ZFMK 97sk216 (flying); P, *Corvus corone* ZFMK 78sk14 (flying); Q, *Dendrocopos major* ZFMK 92sk2 (flying); R, *Fulmarus glacialis* ZFMK 91sk26 (flying, surface swimmer); S, *Uria aalge* ZFMK 75sk74 (amphibious: flying, diving); T, *Dacelo novaeguineae* ZFMK 012sk47 (flying); U, *Larus argentatus* ZFMK 89sk3 (flying, surface swimmer); V, *Alca torda* ZFMK 73sk93 (amphibious: flying, diving).

sion of MESQUITE (Maddison & Maddison, 2014), were already used for these kinds of data (Dumont *et al.*, 2013; Quémeneur *et al.*, 2013) but not the second test, which is probably worthy of brief explaination. This test uses only the direction of the relationship (directly or inversely proportional) between the contrasts of the two characters of interest, rather than performing a linear regression on the contrasts. This has both drawbacks and advantages. The main drawback is that the test generally yields lower power because the magnitude of change in the contrasts is ignored. The principal advantage is that this method should be much more robust to violations of the assumption (shared by PGLS) of the classical FIC method, which is that the characters evolved on the reference tree in accordance with a Brownian motion model of evolution. In the case of our data, this assumption proved unrealistic, as shown by strong artefacts detected in preliminary tests (typically yielding probabilities below 10^{-4} for at least one of the four tests performed on each character; result not shown), and so classical FIC (or PGLS) analysis would have been inadvisable. All our tests (pairwise comparisons and the FIC sign test) use the complete sample.

Effect of body size

Size effects were tested using the same two methods as for the ecological signal, namely pairwise comparisons (Maddison, 2000) and a sign test on FIC (Felsenstein, 1985). In this context, the pairwise comparisons check whether there is a consistent covariation between body size and the microanatomical characters among terminal taxa; the FIC sign test does this at the same time as taking into consideration internal nodes. Again, all our tests (pairwise comparisons and the FIC sign test) use the complete sample, although the FIC sign test is expected to be more powerful precisely because it uses inferred nodal values between which additional comparisons are made. In addition to these phylogeny-informed statistical approaches, simple linear regressions were conducted using PRISM (Graphpad Software Inc.) to better visualize the data, and to quantify the significant relationships involving body size (slope of regressions), as revealed by pairwise comparisons and FIC. Null hypotheses were rejected at a threshold of $P < 0.01$, which represents the standard threshold of $P < 0.05$ adjusted for multiple testing of the present study via the false discovery rate.

RESULTS

Phylogenetic signal

Qualitative observations reveal obvious differences between taxa (Figs 3–9). In squamates, for example, rib structure is generally simple, with compact cortices and a medullary cavity generally devoid of osseous trabeculae, and the transition between both territories is generally abrupt (Figs 3, 4), although this may reflect their small body size to some extent (see below). The shape of cross-sections is subcircular to elliptic. By contrast, mammals and archosaurs display more complex and variable rib inner structures; for example, in terms of the presence, organization, and density of bone trabeculae (Figs 5–9). In addition, the shape of rib shaft is very variable in mammals, from subcircular to elongated and fusiform (Figs 6, 7, 8, 9). Archosaurs have elliptical to fusiform rib cross-sections (Fig. 5). Statistical tests support these observations: most characters reflecting the size and the microanatomy of the ribs display a phylogenetic signal (Table 1).

Ecological signal

Qualitatively, there appear to be differences related to distinct lifestyles in both mammals and birds (Figs 5–9), although exceptions occur, as noted below.

The bats (Fig. 8A–D) exhibit simple bone microanatomy, with thin cortices, and few (if any) slender bone trabeculae in the medullary region, as expected for flying taxa. Only some amphibious mammals pre-

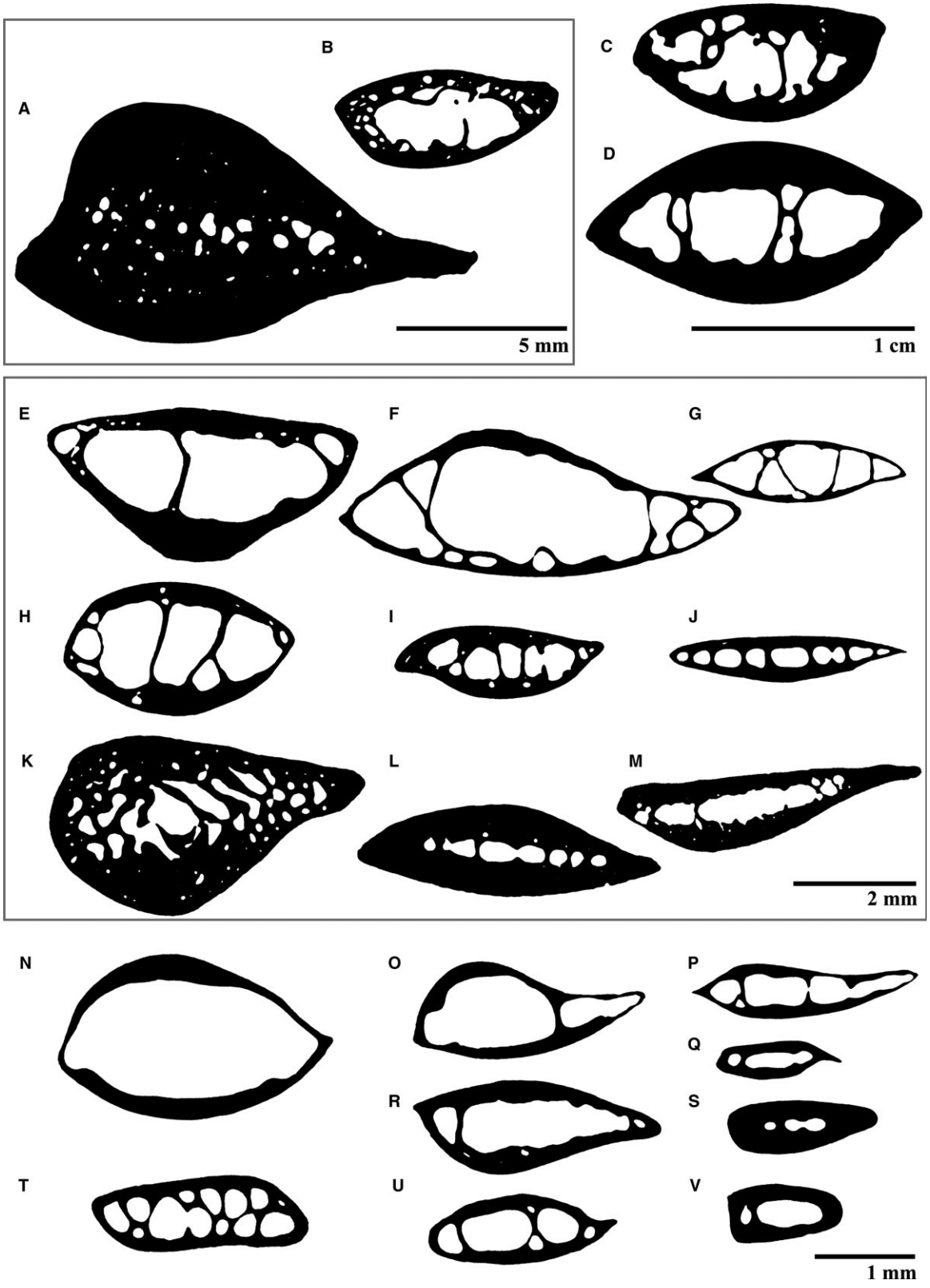
A
B
5 mm
C
D
1 cm
E
F
G
H
I
J
K
L
M
2 mm
N
O
P
Q
R
S
T
U
V
1 mm

Figure 6. Mid-shaft cross-sections of the median ribs of various mammalian species (monotremes: A–C; marsupials: D–G; Paenungulata: H, I; Xenarthra: J, K; primates: L–P; lagomorph: Q; rodents: R–Y; Eulipotyphla: Z-b). The various lifestyles and locomotor patterns are given in brackets. The sections sharing the same scale bar are sometimes delimited by a grey rectangle for clarity. A, *Ornithorhynchus anatinus* AMNH 77856 (amphibious); B, *Tachyglossus aculeatus setosus* AMNH 65833 (terrestrial); C, *Zaglossus bruijni* AMNH 66194 (terrestrial); D, *Perameles nasuta* MHNL 50.00.0989 (terrestrial, fossorial); E, *Didelphis* sp. MHNL 50.00.0917 (terrestrial); F, *Vombatus ursinus* MHNL 50.00.0785 (terrestrial, fossorial); G, *Macropus rufus* MHNL 50.00.0931 (terrestrial); H, *Dugong dugon* MHNL 50.00.2521 (aquatic, shallow/coastal waters); I, *Elephas maximus* MHNL 50.00.2671 (terrestrial); J, *Choloepus didactylus* MNHN-1999.1062 (arboreal); K, *Myrmecophaga tridactyla* MNHN-2005.269 (terrestrial); L, *Cercopithecus mona* ZFMK MAM_1976.0302 (arboreal); M, *Galagoides demidovii* ZFMK MAM_1981.1730 (arboreal); N, *Callithrix jacchus* ZFMK MAM_1983.0366 (arboreal); O, *Gorilla gorilla* MHNL 50.00.1762 (terrestrial); P, *Gorilla gorilla* MHNL 50.00.1751 (terrestrial); Q, *Lepus europaeus* p.c. VB (terrestrial); R, *Dasyprocta punctata* ZFMK MAM_2012.0472 (terrestrial); S, *Myoprocta pratti* ZFMK MAM_2001.0023 (terrestrial); T, *Castor fiber* MHNL 50.00.0788 (amphibious); U, *Myocastor coypus* p.c. VB (amphibious); V, *Rattus norvegicus* p.c. VB (terrestrial); W, *Sciurus vulgaris* ZFMK MAM_1989.0261 (arboreal); X, *Arvicola amphibius* ZFMK MAM_2012.0372 (amphibious); Y, *Apodemus* sp. p.c. VB (terrestrial); Z, *Erinaceus europaeus* p.c. VB (terrestrial); a, *Galemys pyrenaicus* MHNL 50.00.046 (amphibious); b, *Crocidura russula* p.c. VB (terrestrial).

sent thicker cortices (and thus smaller medullary cavities) and, overall, more compact sections than their closest terrestrial relatives. This is the case for the platypus *Ornithorhynchus anatinus* (Fig. 6A), which presents a global compactness of 0.92, whereas both echidnae (Fig. 6B, C) have a rib compactness of 0.64 and 0.52, respectively (see Supporting information, Table S1). The European beaver *Castor fiber* (Fig. 6T) also presents a thicker cortex than most terrestrial rodents (Fig. 6R, S, V). However, two other amphibious rodents, the coypu *Myocastor coypus* (Fig. 6U) and the water vole *Arvicola amphibius* (Fig. 6X), have a cortical thickness similar to that of most terrestrial rodents, except the rat (Fig. 6V), as already reported by de Buffrénil *et al.* (2010). Among perissodactyls, both tapir species categorized as amphibious differ from each other in term of rib compactness, although they do not greatly differ from their terrestrial relatives, such as horses. Thus, *Tapirus terrestris* (Fig. 8G) shows a higher global compactness (0.76) than its sister species *Tapirus indicus* (0.58) (Fig. 8F), whereas the horse (Fig. 8E) displays an intermediate value (0.68). Both species of hippos (Fig. 9A, B) have thicker cortices and higher compactness values than terrestrial cetartiodactyls (Fig. 8J–T). Among the carnivores, the polar bear *Ursus maritimus* (Fig. 8H), also categorized as amphibious, does not exhibit thicker cortices than its terrestrial relatives. Species living in shallow water or coastal environments, such as the sea otter *Enhydra lutris* (Fig. 7E), some pinnipeds (Fig. 7K–P), some cetaceans (Fig. 9C, D, F, G), and the dugong (Fig. 6H), exhibit variable global compactness values ranging from 0.54 to 0.98. Except for the walrus *Odobenus rosmarus* (Fig. 7O), the harbour seal *Phoca vitulina* (Fig. 7K), and the Amazon River dolphin *Inia geoffrensis* (Fig. 9F), these animals show moderately to considerably thicker cortices or global compactness values than their terrestrial relatives. Three out of the five mammalian species categorized as aquatic deep divers exhibit an osteoporotic-like bone structure, with rather thin compact cortices and most of the section consisting of a spongiosa made of thin but numerous bone trabeculae. This is best represented by the hooded seal *Cystophora cristata* (Fig. 7Q) and Blainville's beaked whale *Mesoplodon densirostris* (Fig. 9E). However, both monodontids *Delphinapterus leucas* (Fig. 9H) and *Monodon monoceros* (Fig. 9J) sampled in the present study exhibit unexpected thick cortices and thicker bone trabeculae in the medullary region. Both species considered as having a fossorial behaviour in our mammalian sample, namely the wombat *Vombatus ursinus* (Fig. 6F) and the long-nosed bandicoot *Perameles nasuta* (Fig. 6D), exhibit relatively thicker bone cortices than their closest terrestrial relative sampled in the present study, the opossum *Didelphis* sp. (Fig. 6E), although these are not thicker than the cortex of the red kangaroo *Macropus rufus* (Fig. 6G). Finally, *Rhinoceros sondaicus* (Fig. 8H) exhibits unusually thick cortices and a high global compactness value for a terrestrial mammal.

In birds, there is a tendency towards an increase in cortical thickness (represented by parameter *P*) and global compactness (*Comp.*) when comparing flying species, terrestrial species, and taxa specialized in diving (Figs 5, 10). As observed for bats, flying birds (including surface-swimming species and unspecialized divers), present very thin compact cortices with large open medullary cavities occupied by no or few slender trabeculae. This is best illustrated by the pelican *Pelecanus* sp. (*Comp.* = 0.26; Fig. 5F), the mallard *Anas plathyrhynchos* (*Comp.* = 0.32; Fig. 5G) or the common buzzard *Buteo buteo* (*Comp.* = 0.29; Fig. 5N). Some birds categorized as

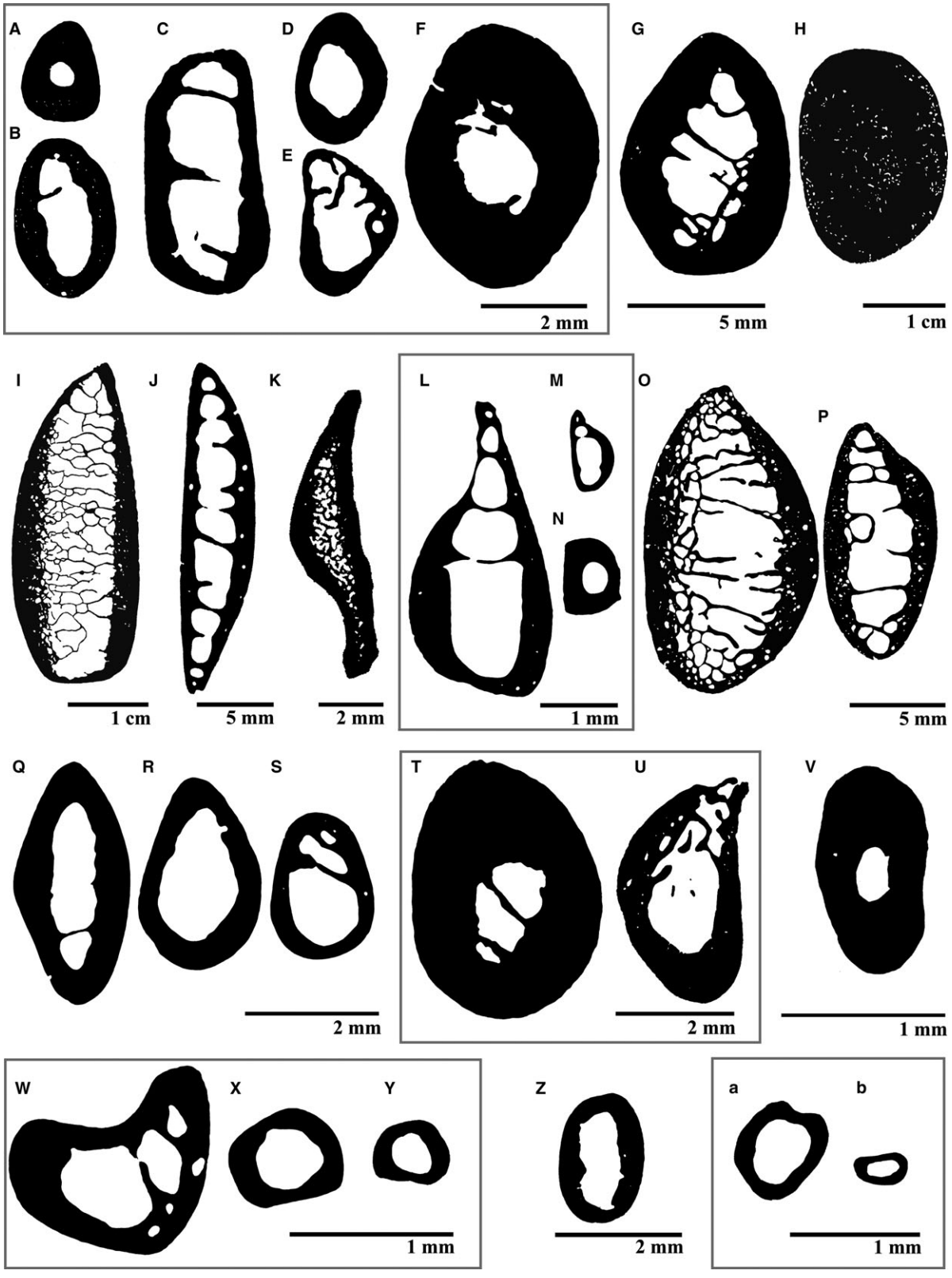
A
B
C
D
E
F
2 mm
G
5 mm
H
1 cm
I
1 cm
J
5 mm
K
2 mm
L
M
N
1 mm
O
P
5 mm
Q
R
S
2 mm
T
U
2 mm
V
1 mm
W
X
Y
1 mm
Z
2 mm
a
b
1 mm

flying in our sample nonetheless display higher rib compactness values, such as the great bustard *Otis tarda* (*Comp*. = 0.46; Fig. 5E) or the laughing kookaburra *Dacelo novaeguineae* (*Comp*. = 0.57; Fig. 5T). Terrestrial birds, represented in the present study by the Southern cassowary *Casuarius casuarius* (Fig. 5C) and the ostrich *Struthio camelus* (Fig. 5D), have thicker cortices than most flying birds, with a mean global compactness of 0.63. Birds that fly and dive when foraging, such as the great cormorant *Phalacrocorax carbo* (Fig. 5I), present very variable rib compactness values (or parameter *P*; Fig. 10) but with a mean compactness higher than most flying and terrestrial birds. Finally, the three flightless diving birds (Fig. 5K, L, M) present thick cortices and reduced medullary cavities (high *Comp*. values and low parameter *P* values; Fig. 10).

Among the crocodiles classified as amphibious, *Crocodylus niloticus* exhibits very compact ribs with almost no medullary cavity and a thick cortex (Fig. 5A). Its closest relative, the dwarf crocodile *Osteolaemus tetraspis* (Fig. 5B), shows a wide medullary cavity and thinner cortices.

Rib microanatomy is rather homogeneous between lepidosaurs of different lifestyles (Figs 3, 4). There is no clear difference in rib microanatomy between limbed and limbless squamate species.

The FIC sign test did not detect any ecological signal (one positive result was found for *LG*, although it is no longer significant after correction for multiple tests), whereas pairwise comparisons found a significant effect on *P*, P_{rad}, and global compactness (Table 2). These effects were stronger on our preferred coding of lifestyle into eight states than in other schemes tested. For example, the relationship with P_{rad} has an associated probability of 0.0009 with our preferred coding (Table 2), but the probability is 0.0068 with our original coding (into ten states) and, if we greatly simplify into a ternary coding similar to that used in most of our previous studies (0, flying, arboreal, fossorial, and terrestrial; 1, amphibious; 2, aquatic), the probability increases further to 0.1051 and is no longer significant.

Effect of body size

Qualitatively, there appear to be differences in rib inner structure between small and large animals. The rib shaft in taxa of large body size tends to show a more complex organization, with an increased transition zone between compact cortex and medullary cavity, often characterized by the presence of bone trabeculae. Thus, the Komodo dragon *Varanus komodoensis* (Fig. 3F) is the largest extant lepidosaur and its inner rib structure is more complex than that of all other closely related taxa (Fig. 3). This pattern is also observable in mammals: most taxa with *MD* < 5 mm and *LG* inferior to approximately 100 mm, such as small primates (Fig. 6L–N), rodents and lagomorphs (Fig. 6Q–Y), carnivores (e.g. small mustelids or viverrids, Fig. 7A–D), bats (Fig. 8A–D), and the Eulipotyphla (Fig. 6Z–b), have a rather simple bone structure with, in most cases, a clear transition between medullary cavity and compact cortex, and no or few bone trabeculae. Conversely, larger species tend to have more complex rib structures, with numerous bone trabeculae occupying the medullary region, as exemplified by medium-sized to large carnivores (Fig. 7I–Q), perissodactyls (Fig. 8E–I), and cetartiodactyls (Figs 8J–T, 9). This is clearly illustrated among primates by the difference between the gorilla (Fig. 6O, P) and smaller forms (Fig. 6L–N).

Our statistical analyses reveal an impact of size on rib microanatomy (Table 3) but only with the FIC sign test; the pairwise comparisons detected no relationship, presumably reflecting the lower power of this method when used on continuous data. Of the three characters that reflect rib size, rib length (*LG*) has the least effect. Maximal diameter (*MD*) and rib *Area* appear to have the strongest effect on rib microanatomy because they both affect several characters, especially *Min*, *S*, Min_{rad}, SD (Min_{rad}), and SD (P_{rad}). The three parameters containing an ecological signal (*P*, P_{rad}, and global compactness) do not appear to be affected by rib size (Table 3).

Simple linear regressions (Fig. 11, Table 4) were conducted for three parameters *Min*, Min_{rad}, and *S*, with cross-section *Area* or *MD* as the independent variable, to illustrate the covariation between these characters. In all cases, the slope of the regression line is undoubtedly different from zero ($P < 0.0001$) but r^2 is relatively low in general. As already shown by the FIC analyses, *S*, *Min*, and Min_{rad} increase with size. It is interesting to note, for example, that two Min_{rad} values are clearly far above the regression line (Fig. 12B): that of the sea otter *Enhydra lutris* (0.527) and that of *Dugong dugon* (0.970). Both of these taxa inhabit shallow coastal waters. If they are excluded from the regression, then r^2 value increases sensibly (0.428 vs. 0.284).

DISCUSSION

Phylogenetic signal

We found a phylogenetic signal in most compactness profile parameters. This was expected because previous studies found similar results for the microanatomy of long bones and vertebrae in amniotes (Cubo *et al.*, 2005; Canoville & Laurin, 2010; Dumont *et al.*, 2013; Quémeneur *et al.*, 2013; Houssaye *et al.*, 2014).

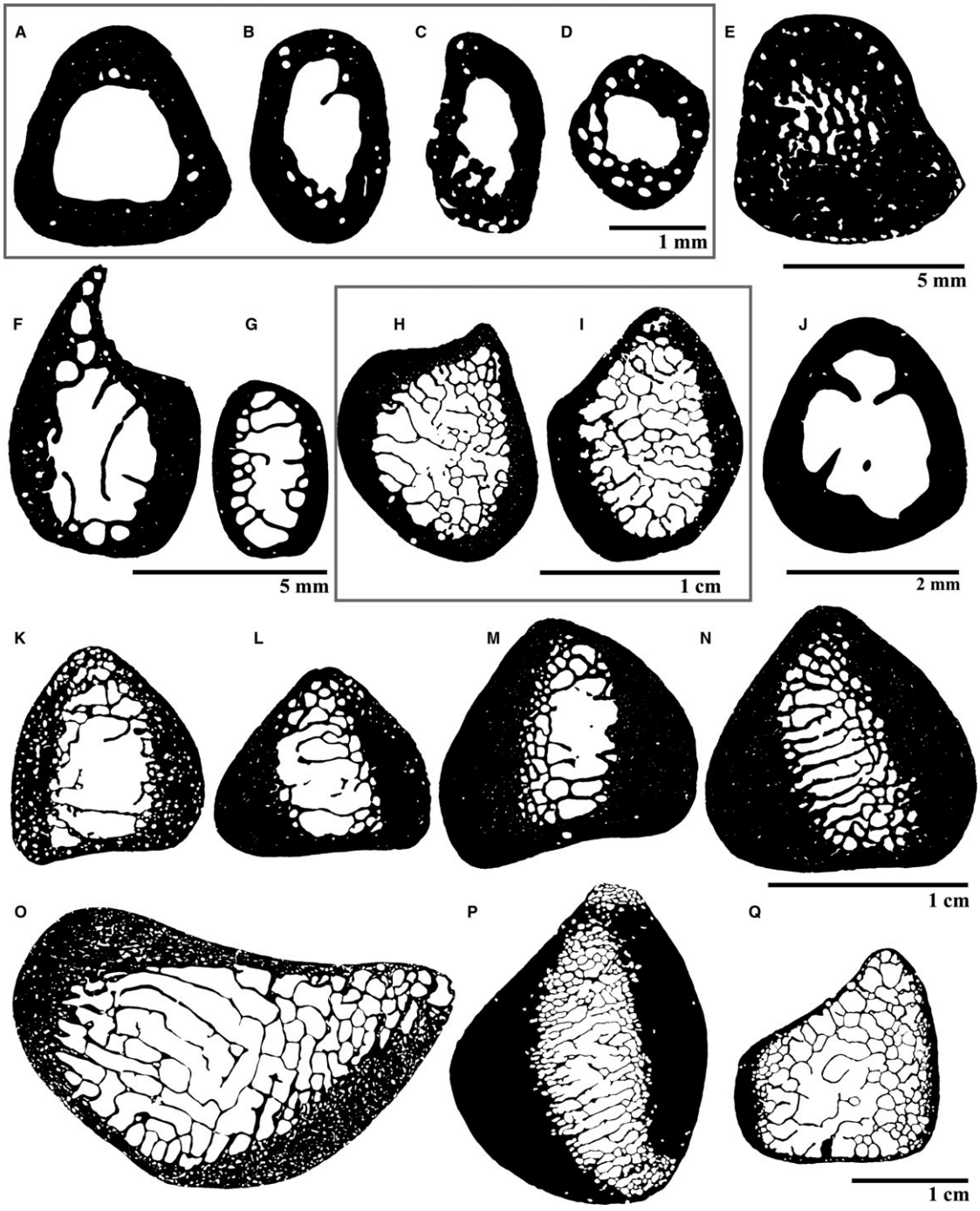

Figure 7. Mid-shaft cross-sections of the median ribs of carnivoran mammals. The various lifestyles and locomotor patterns are given in brackets. The sections sharing the same scale bar are sometimes delimited by a grey rectangle for clarity. A, *Martes martes* p.c. VB (arboreal, terrestrial); B, *Martes foina* p.c. VB (arboreal, terrestrial); C, *Neovison vison* p.c. VB (amphibious); D, *Genetta genetta* p.c. VB (arboreal, terrestrial); E, *Enhydra lutris* MHNL 50.00.1023 (Aquatic, shallow/coastal waters); F, *Canis lupus* p.c. VB (terrestrial); G, *Vulpes vulpes* p.c. VB (terrestrial); H, *Ursus maritimus* p.c. VB (amphibious); I, *Panthera leo persica* AMNH 54995 (terrestrial); J, *Felis silvestris* p.c. VB (terrestrial); K, *Phoca vitulina* MHNL 50.00.1020 (aquatic, shallow/coastal waters); L, *Monachus monachus* MHNL 50.00.1018 (aquatic, shallow/coastal waters); M, *Zalophus californianus* AMNH 63946 (aquatic, shallow/coastal waters); N, *Arctocephalus pusillus* AMNH 81701 (aquatic, shallow/coastal waters); O, *Odobenus rosmarus* MHNL 50.00.1014 (aquatic, shallow/coastal waters); P, *Eumetopias jubatus* AMNH 38400 (aquatic, shallow/coastal waters); Q, *Cystophora cristata* AMNH 184659 (aquatic, deep diver).

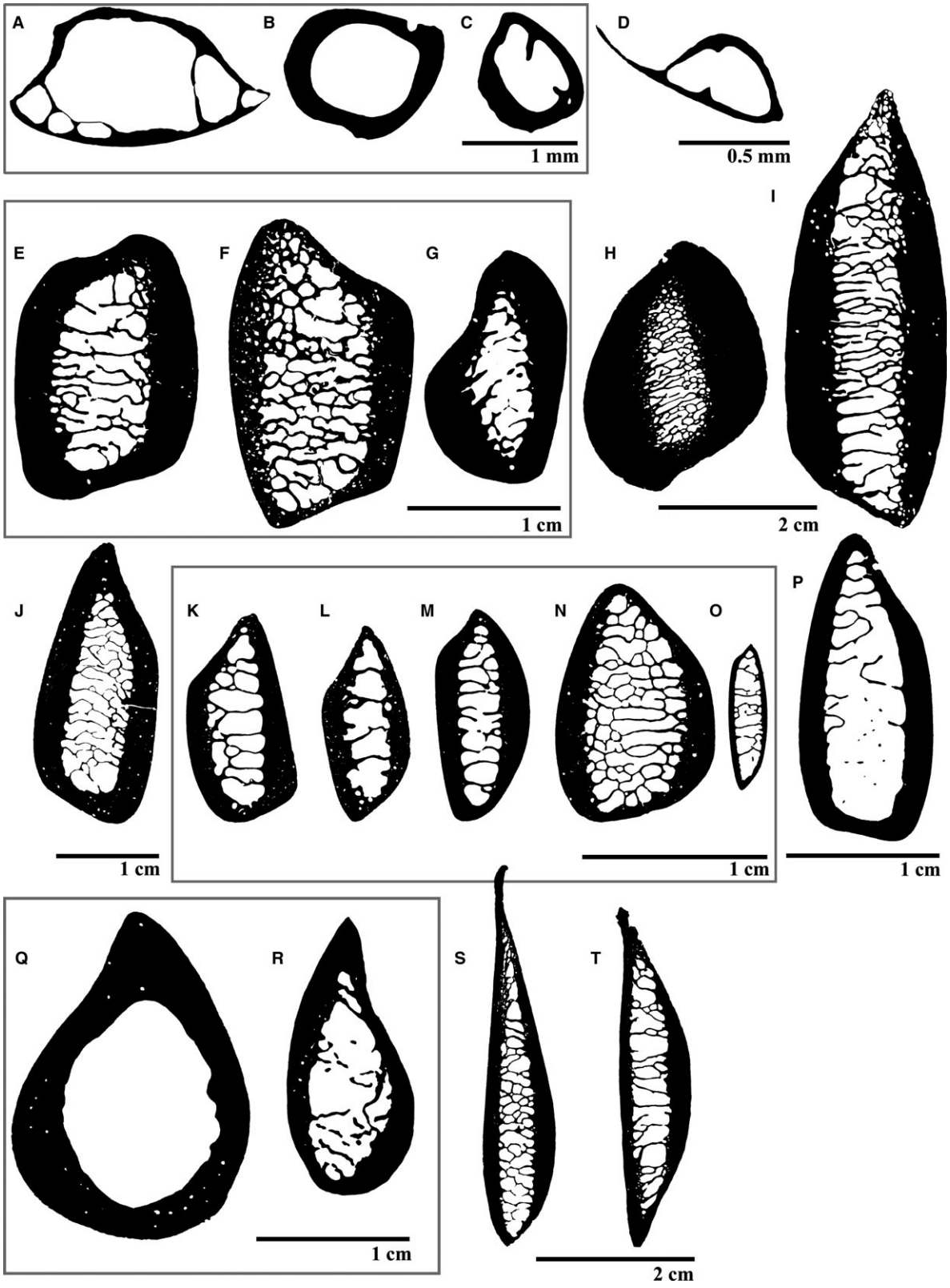
A
B
C
1 mm
D
0.5 mm
E
F
G
1 cm
H
I
2 cm
J
1 cm
K
L
M
N
O
1 cm
P
1 cm
Q
R
1 cm
S
T
2 cm

Figure 8. Mid-shaft cross-sections of the median ribs of various mammalian species (bats: A–D; perissodactyls: E–I; cetartiodactyls: J–T). The various lifestyles and locomotor patterns are given in brackets. The sections sharing the same scale bar are sometimes delimited by a grey rectangle for clarity. A, *Pteropus giganteus* ZFMK 80.851 (flying); B, *Eidolon helvum* ZFMK no sp. number (flying); C, *Rousettus aegyptiacus* ZFMK 2001.004 (flying); D, *Pipistrellus pipistrellus* ZFMK a (flying); E, *Equus caballus* MHNL 50.00.2029 (terrestrial); F, *Tapirus indicus* MHNL 50.00.2038 (amphibious); G, *Tapirus terrestris* ZFMK field no. 418 (amphibious); H, *Rhinoceros sondaicus* MHNL 50.00.2041 (terrestrial); I, *Ceratotherium sinum* AMNH 51855 (terrestrial); J, *Bison bison* MHNL 50.00.2450 (terrestrial); K, *Ovis aries* p.c. VB (terrestrial); L, *Hemitragus jayakari* p.c. VB (terrestrial); M, *Aepyceros melampus* p.c. VB (terrestrial); N, *Sus scrofa* p.c. VB (terrestrial); O, *Capreolus capreolus* p.c. VB (terrestrial); P, *Cervus elaphus canadensis* MHNL 50.00.2211 (terrestrial); Q, *Giraffa camelopardalis* MHNL 50.00.2060 (terrestrial); R, *Giraffa camelopardalis* MHNL 50.00.2061 (terrestrial); S, *Camelus dromedarius* MHNL 50.00.2063 (terrestrial); T, *Camelus bactrianus* MHNL 50.00.2066 (terrestrial).

Squamates, for example, have a generalist tubular rib structure, which is different from most archosaurs and mammals. Moreover, most snakes exhibit very uniform bone architecture, regardless of their lifestyle adaptation. This was already observed for the internal structure of the vertebrae in extant snakes (de Buffrénil & Rage, 1993; Houssaye *et al.*, 2010, 2013, 2014). Our results suggest that different taxonomic groups (lepidosaurs, archosaurs, mammals) exhibit different adaptive responses to their environment, and are perhaps affected by slightly different inherent structural constraints.

Ecological signal

The significant effect of lifestyle on P, P_{rad}, and global compactness (Table 2) means that changes in lifestyle are accompanied by changes in the cortical thickness of the ribs, rather than the extent of the spongiosa. The negative relationship with P and P_{rad} indicates that the ribs of taxa scored with a higher lifestyle number (coastal swimmers inhabiting shallow waters is the highest lifestyle category) have a smaller medullary cavity than taxa scored with a low number (flying is the lowest). The positive relationship with global compactness would reflect the same phenomenon, given that compactness reflects mostly the size of the medullary cavity in our sample; cortical compactness is uniformly high, and *Min* (compactness of the medullary spongiosa, if present) is more variable, although it does not appear to covary with lifestyle in our sample. All of these conclusions prevail even if lifestyle is recoded into a binary variable (aquatic taxa vs. others; results not shown). These results confirm our working hypothesis that the ribs are partly involved in the inertia and density of the body and that flying taxa, for example, have lighter skeletons overall and thus lighter ribs, than terrestrial or aquatic ones.

It is possible that the relatively low number of significant relationships found with habitat (lower than for rib size) reflects the following methodological problems:

1. The FIC sign test and pairwise comparisons assume that the states are linearly and correctly ordered in a way that is coherent with the value of the dependent (microanatomical and size) characters. Although we ordered the states according to our ideas of how each lifestyle should influence rib compactness, and performed some exploratory analyses to verify the relevance of our ordering scheme, we could not test all possibilities [i.e. ordering states a posteriori into the scheme yielding the greatest correlation with other variables would have been invalid (i.e. a circular procedure) and so this was not carried out]. It is conceivable that another coding of lifestyle would have led to the detection of more lifestyle effects on rib structure. This problem may be more acute in the present study than in most of our earlier studies because we coded a greater number of lifestyle categories, thus creating smaller subsamples for each of the categories (most of our previous studies considered lifestyle as a ternary variable; e.g. Kriloff *et al.*, 2008; Canoville & Laurin, 2010; Quémeneur *et al.*, 2013).
2. Lifestyle was coded as a discrete variable. This coding is less informative than quantitative data about habitat use (e.g. proportion of time spent in trees, in water, on land, flying, the depth at which the taxon is most active, etc.). However, data concerning such quantitative habitat use are currently unavailable for most of the sampled taxa.
3. For practical reasons, we had to assign each species to a single lifestyle category, which is not optimal because some animals are generalist and occupy various habitats. For example, many squamates, such as some varanids, are good runners and climbers, although they also spend a fair amount of time in water, and can quickly dig large, extensive burrows. Moreover, numerous semi-aquatic mammals, such as the coypu *M. coypus*, the European water vole *A. amphibius*, and the platypus *O. anatinus*, are also semi-fossorial or fossorial.

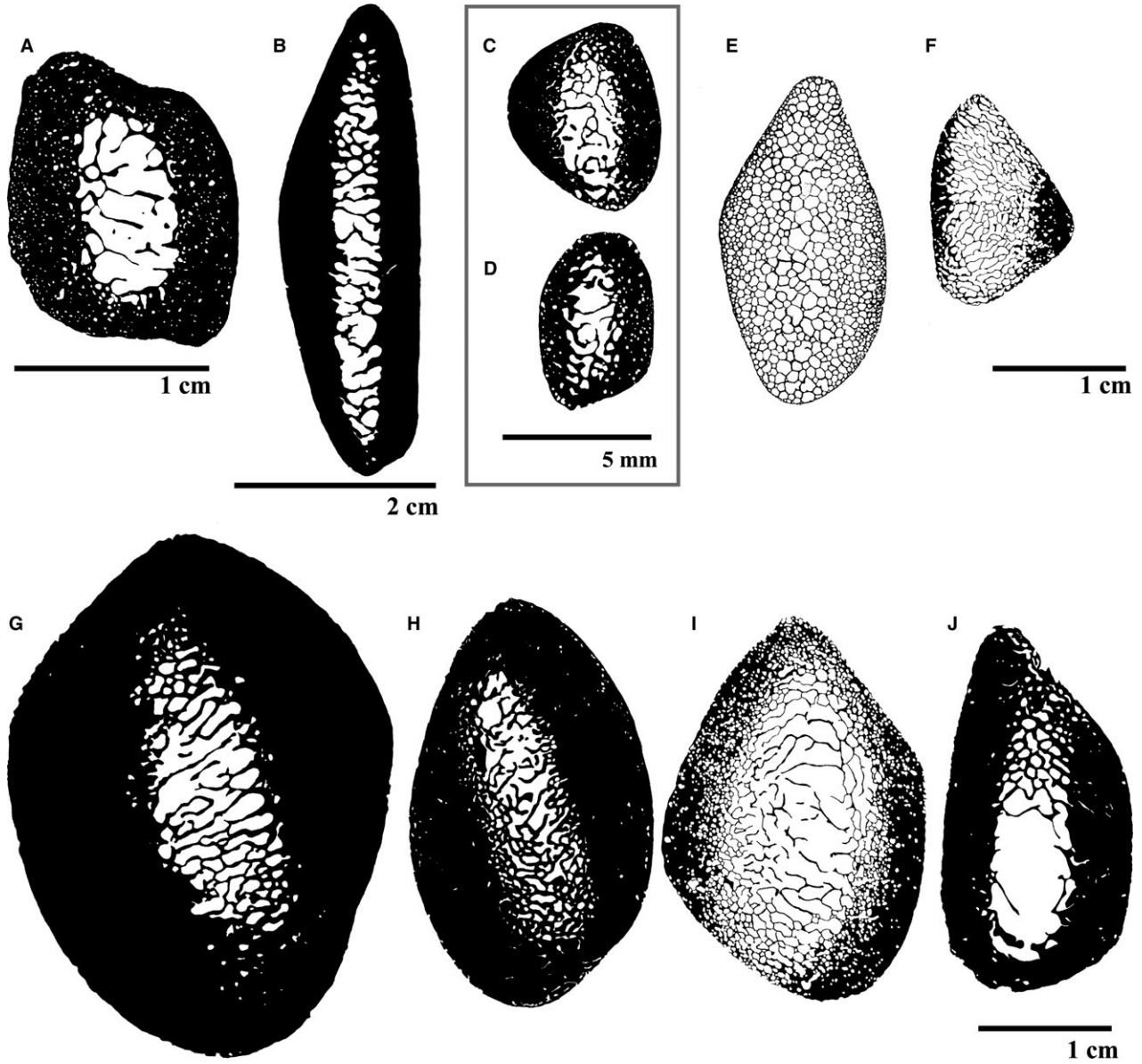

Figure 9. Mid-shaft cross-sections of the median ribs of various cetartiodactyl species (hippopotamids: A, B; cetaceans: C–J). The various lifestyles and locomotor patterns are given in brackets. The sections sharing the same scale bar are sometimes delimited by a grey rectangle for clarity. A, *Choeropsis liberiensis* AMNH 148452 (amphibious); B, *Hippopotamus amphibius* MHNL 50.00.2123 (amphibious); C, *Phocoena phocoena* MHNL 50.00.1046 (aquatic, shallow/coastal waters); D, *Lissodelphis borealis* AMNH 31422 (aquatic, shallow/coastal waters); E, *Mesoplodon densirostris* AMNH 139931 (aquatic, deep diver); F, *Inia goeffrensis* AMNH 209101 (aquatic, shallow/coastal waters); G, *Orcinus orca* AMNH 34261 (aquatic, shallow/coastal waters); H, *Delphinapterus leucas* AMNH 34936 (aquatic, deep diver); I, *Globicephala melas* AMNH 215271 (aquatic, deep diver); J, *Monodon monoceros* MHNL 50.00.1027 (aquatic, deep diver).

4. The definition of some lifestyle categories may be too broad and encompass taxa with quite distinct ecologies. This is probably the case for taxa categorized as 'amphibious' in the present study. Indeed, this class includes species with a wide range of habitat preferences and diverse swimming modes (Fish, 1996). Thus, although some species spend more time on dry land than in water (such as the tapirs), others spend most of their time in water (such as the common hippo). Moreover, some species may favour submerged swimming, whereas others usually stay at the surface, and a bone mass increase would be disadvantageous to the latter. This probably

Table 1. Phylogenetic signal in the rib size and microanatomical data

Character	*P*-values
Discrete characters	
Habitat (unordered)	**< 0.0001***
Habitat (ordered)	**< 0.0001***
Continuous characters	
LG	**< 0.0001***
MD	**< 0.0001***
Area (mm^2)	0.1843
Min	**0.0077***
Max	0.9323
S	**< 0.0001***
P	**< 0.0001***
Min_{rad}	**0.0328**
SD (Min_{rad})	**0.0017***
Max_{rad}	0.7006
SD (Max_{rad})	0.1259
S_{rad}	**0.0488**
SD (S_{rad})	**< 0.0001***
P_{rad}	**0.0002***
SD (P_{rad})	**< 0.0001***
Comp.	**< 0.0001***

Significant results are indicated in bold; those that remain significant after correction for multiple tests are indicated by an asterisk. *Comp.*, global compactness; *LG*, rib global length; *MD*, maximal diameter of the cross-section.

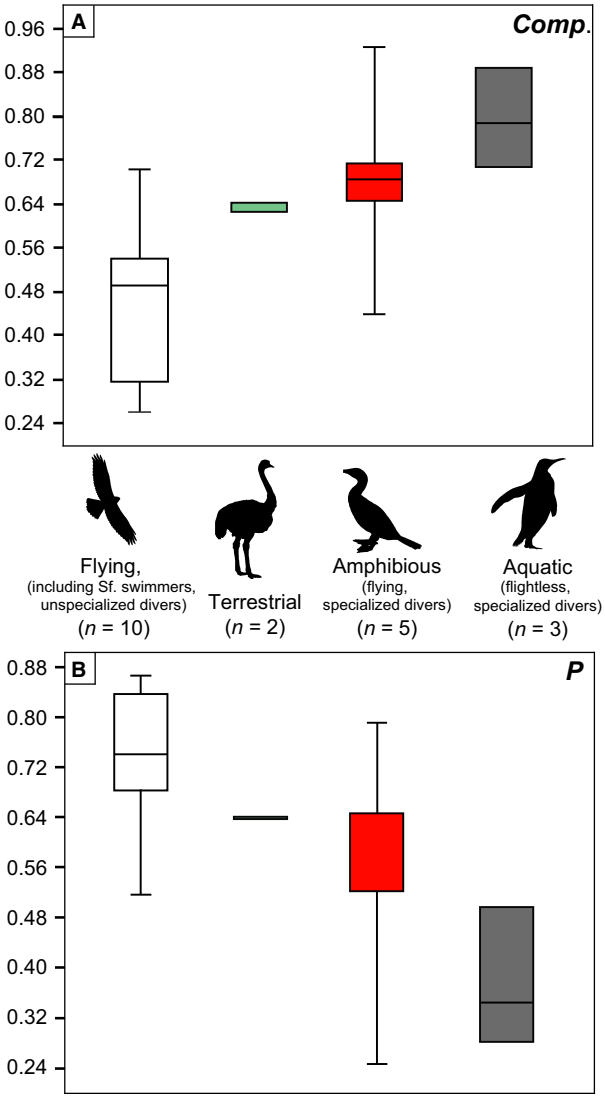

Figure 10. Descriptive statistics of the various lifestyle categories (flying; terrestrial; amphibious; aquatic) of the birds in our sample ($N = 20$) for global compactness (*Comp.*) in (A), and parameter *P* in (B). Unfortunately, the bird sample size is too small to perform meaningful phylogeny-informed statistical tests, and so this illustration should only be considered as an exploratory analysis.

explains the great variability in rib compactness among the species categorized in the present study as amphibious. In mammals, for example, the pigmy hippo *Choeropsis liberiensis* exhibits thinner bone walls and a lower global compactness than its closest relative the common hippo *Hippopotamus amphibius*. This difference was also observed in the long limb bones of these species (Wall, 1983; Houssaye *et al.*, 2015b) and can be explained by the fact that the pygmy hippo spends considerably less time in water, and is thus more terrestrial than *H. amphibius* (Eltringham, 1993). Similarly, the Malayan tapir *T. indicus* is the least aquatic of the extant Tapiridae and presents a lower rib compactness value than *T. terrestris*. For the archosaurs, the dwarf crocodile *O. tetraspis* is the least aquatic African crocodile (Luiselli, Akani & Capizzi, 1999) and shows a lower compactness value in the ribs than the Nile crocodile. Among birds, the species categorized as amphibious (i.e. that fly but also dive) also show a broad range of rib compactness values (Fig. 10). However, this group again includes species with different ecologies and locomotion modes underwater. Previous studies have highlighted the difficulty of discriminating between amphibious and terrestrial taxa on the basis of long bone microanatomy (Canoville & Laurin, 2009, 2010; Quémeneur *et al.*, 2013).

5. Our results could also be affected by the standardized sampling location chosen in this exploratory study. Indeed, we restricted our observations to the mid-shaft of the median rib in the thoracic rib series. However, as noted above, for a single individual, bone microanatomy can vary along the rib series and within a

Table 2. Ecological signal in the rib microanatomical and size data

Character	*P*-values (FIC)	*P*-values (PC)	Sign
LG	**0.0192**	0.2219	
MD	0.1705	0.1619	
Area (mm^2)	0.1255	0.1619	
Min	0.6908	0.1133	
Max	0.7520	0.5000	
S	0.4684	0.3523	
P	0.2576	**0.0009***	–
Min_{rad}	0.9204	0.1133	
SD (Min_{rad})	0.8424	0.3770	
Max_{rad}	0.7843	0.5000	
SD (Max_{rad})	0.9273	0.5000	
S_{rad}	0.6110	0.1977	
SD (S_{rad})	0.3594	0.1917	
P_{rad}	0.2917	**0.0009***	–
SD (P_{rad})	0.4189	0.4225	
Comp.	0.0903	**0.0035***	+

The independent character is lifestyle with eight states (best coding). Two phylogeny-informed tests were used: the phylogenetic independent contrast in sign test version (because statistical artefacts prevented the regression-based test) and pairwise comparisons. Significant results are shown in bold; those that remain significant after correction for multiple tests are indicated by an asterisk. The sign of the relationship is indicated only when it is statistically significant (before correction for multiple tests). *Comp*., global compactness; FIC, Felsenstein independent contrasts analysis, sign test; *LG*, rib global length; *MD*, maximal diameter of the cross-section; PC, pairwise comparisons analysis.

single element from the proximal to the distal end (Waskow & Sander, 2014). Previous studies have shown that the different ribs of the rib series are subject to contrasted mechanical stresses (e.g. as a result of locomotion or posture: Fujiwara *et al.*, 2009; Casha *et al.*, 2015b), which is likely to affect their cortical thickness (Casha *et al.*, 2015b). Lifestyle adaptations could also affect preferentially certain zones of the rib series depending on the taxa considered. Indeed, Houssaye (2013: fig. 20) showed that the distribution of bone mass increase (associated with an aquatic lifestyle) along the axial skeleton is variable between species of extinct marine squamates. Future research should aim to explain and quantify inter- and intraspecific variability in rib microanatomy along the rib series and within a single element to determine whether a general pattern can be recognized among phylogenetically close taxa or animals sharing similar locomotor behaviours or habitat preferences.

6. Finally, the influence of the physiological status of our specimens at the time of death must be considered. A temporary deficiency in calcium, for example, can induce bone resorption and result in a decrease in measured bone compactness. Ontogenetic age is also known to severely bear on bone volume, especially in female individuals (de Buffrénil & Francillon-Vieillot, 2001; Heinrich, 2015). Because most taxa included in the sample are represented by one specimen only, the effects of such factors cannot be excluded entirely.

Rib microanatomy in some groups differs from our predictions. Cetaceans are remarkable in this respect because they display a great variability in rib compactness. As predicted, some coastal cetaceans, such as the killer whale *Orcinus orca*, indeed show compact cortices, and some deep divers, such as the Blainville's beaked whale *M. densirostris*, exhibit osteoporotic-like ribs. However, neither the beluga *D. leucas*, nor the narwhal *M. monoceros*, which are categorized as pelagic deep divers, exhibit the expected osteoporotic condition; instead, they have rather thick compact cortices. This observation could be explained, at least for the beluga, by its variable lifestyle habits, alternatively inhabiting deep-water environments or more coastal habitats through the year (Heide-Jørgensen, Richard & Rosing-Asvid, 1998). This characteristic could also represent a phylogenetic peculiarity specific to the Monodontidae. The Amazon River dolphin, *I. geoffrensis*, inhabits shallow water environments but exhibits an unexpected, spongy section, with a low global compactness and numerous thin bone trabeculae. This pattern could be specific to fresh water dolphins that are morphologically different from other marine cetaceans, perhaps in part because of their ecological specializations (Martin & Silva, 2004). A similar singularity has also been observed for the vertebral microanatomy of two other river dolphins, *Pontoporia* and *Platanista* (Dumont *et al.*, 2013).

So far, our cetacean rib sample ($N = 8$) is too small to fully explain the relationship between lifestyle and rib inner structure in this mammalian taxon. However, rib microanatomy in cetaceans does not appear to be influenced by lifestyle in the same manner as the appendicular skeleton, a phenomenon already observed in the common dolphin *Delphinus delphis* (de Buffrénil, Sire & Schoevaert, 1986). Previous studies have shown that most extant cetaceans have rather osteoporotic limb bones and vertebrae with rather spongy cross-sections and thin compact cortices (de Buffrénil *et al.*, 1986; de Ricqlès & de Buffrénil, 2001; Canoville & Laurin, 2010; Dumont

Table 3. Impact of size on rib microanatomical data

	Independent character								
	LG (rib length)			*MD* (maximal diameter of the section)			*Area* of the section (mm^2)		
Dependent character	*P*-values (FIC)	*P*-values (PC)	Sign	*P*-values (FIC)	*P*-values (PC)	Sign	*P*-values (FIC)	*P*-values (PC)	Sign
Min	0.2323	0.3804		**0.0460**	0.5000	+	**0.0027***	0.1802	+
Max	1.0000	0.3145		0.9161	0.5000		0.9161	0.5000	
S	**0.0436**	0.4238	+	**2.6142×10^{-4}***	0.4423	+	**0.0122**	0.2762	+
P	0.7465	0.5000		0.9999	0.2516		0.8716	0.3277	
Min_{rad}	0.1933	0.5000		**0.0120**	0.2664	+	**4.0878×10^{-4}***	0.0586	+
SD (Min_{rad})	0.0728	0.5000		**0.0093***	0.5000	+	**0.0051***	0.3776	+
Max_{rad}	0.0548	0.5561		**0.0221**	0.4439	–	0.0548	0.5561	
SD (Max_{rad})	**0.0353**	0.5000	+	0.0548	0.5000		**0.0353**	0.5000	+
S_{rad}	0.0895	0.5000		**0.0172**	0.4901	+	0.0616	0.4901	
SD (S_{rad})	0.0798	0.5489		0.1563	0.4511		0.2112	0.4511	
P_{rad}	0.8078	0.4460		1.0000	0.3277		0.6852	0.3277	
SD (P_{rad})	0.1056	0.5000		**0.0095***	0.5000	+	**0.0058***	0.3244	+
Comp.	0.9358	0.4820		0.9358	0.3607		1.0000	0.4730	

The same two tests as in Table 2 were used. Significant results are shown in bold; those that remain significant after correction for multiple tests are indicated by an asterisk. The sign of the relationship (+/–) is indicated only when it is statistically significant (before correction for multiple tests). *Comp.*, global compactness; FIC, Felsenstein independent contrasts analysis, sign test; *LG*, rib global length; *MD*, maximal diameter of the cross-section; PC, pairwise comparisons analysis.

et al., 2013). Interspecific variability of rib microanatomy in cetaceans could reflect subtle ecological adaptations. Further research with a larger taxonomic sample is needed to understand the cause of this variability.

Body size

Body size, as expressed in the present study by sectional *Area* or *MD*, has a fairly strong impact on rib microanatomy. This is not surprising because many skeletal features (including microanatomical ones) are known to display allometry with body size (Houssaye *et al.*, 2015b), which itself varies by several orders of magnitude within amniotes. The positive relationship between *S* and body size (i.e. *MD*) (Fig. 11C) suggests that the transition zone between cortex and medulla increases in relative width with body size (and particularly rib bulk). This presumably reflects a greater development of the spongiosa in large taxa (such as *Ceratotherium sinum* or *H. amphibius*) (Fig. 11C). This latter relationship is also supported by an increase of *Min* and Min_{rad} values with *Area* (Fig. 11A, B; Tables 3, 4). Thus, there is obviously a pattern of increasing development of medullary spongiosa with body size in the ribs. Our results suggest that small animals have low trabecular complexity and fewer trabeculae than larger animals. Indeed, even though this was not quantified in the present study, small amniotes not only appear to have, when present, fewer trabeculae, but also fewer trabecular connections than large animals. Such a pattern was previously observed in the epiphyses and midshaft of long limb bones and ribs of mammals (Swartz, Parker & Huo, 1998; Houssaye *et al.*, 2015b) and in the vertebrae of mammals and squamates (Dumont *et al.*, 2013; Houssaye *et al.*, 2014). Thus, as for the vertebrae (Dumont *et al.*, 2013; Houssaye *et al.*, 2014), rib internal organization appears to be strongly influenced by body size.

Statistical considerations

Effects of lifestyle on rib microanatomy were detected only by pairwise comparisons, whereas rib size effects on microanatomy were detected by the FIC sign test and simple linear regressions but not pairwise comparisons. Given the number of results involved, this is unlikely to result from random distribution of the significant results. Rather, this must reflect the nature of the characters and methods. Thus, pairwise comparisons handle discrete characters (such as lifestyle) as such. By contrast, the FIC sign test treats these discrete characters as if they were continuous variables, which appears to result in a loss of power. This is logical given that we ordered the lifestyle states according to the expected compactness gradient, rather than the order in

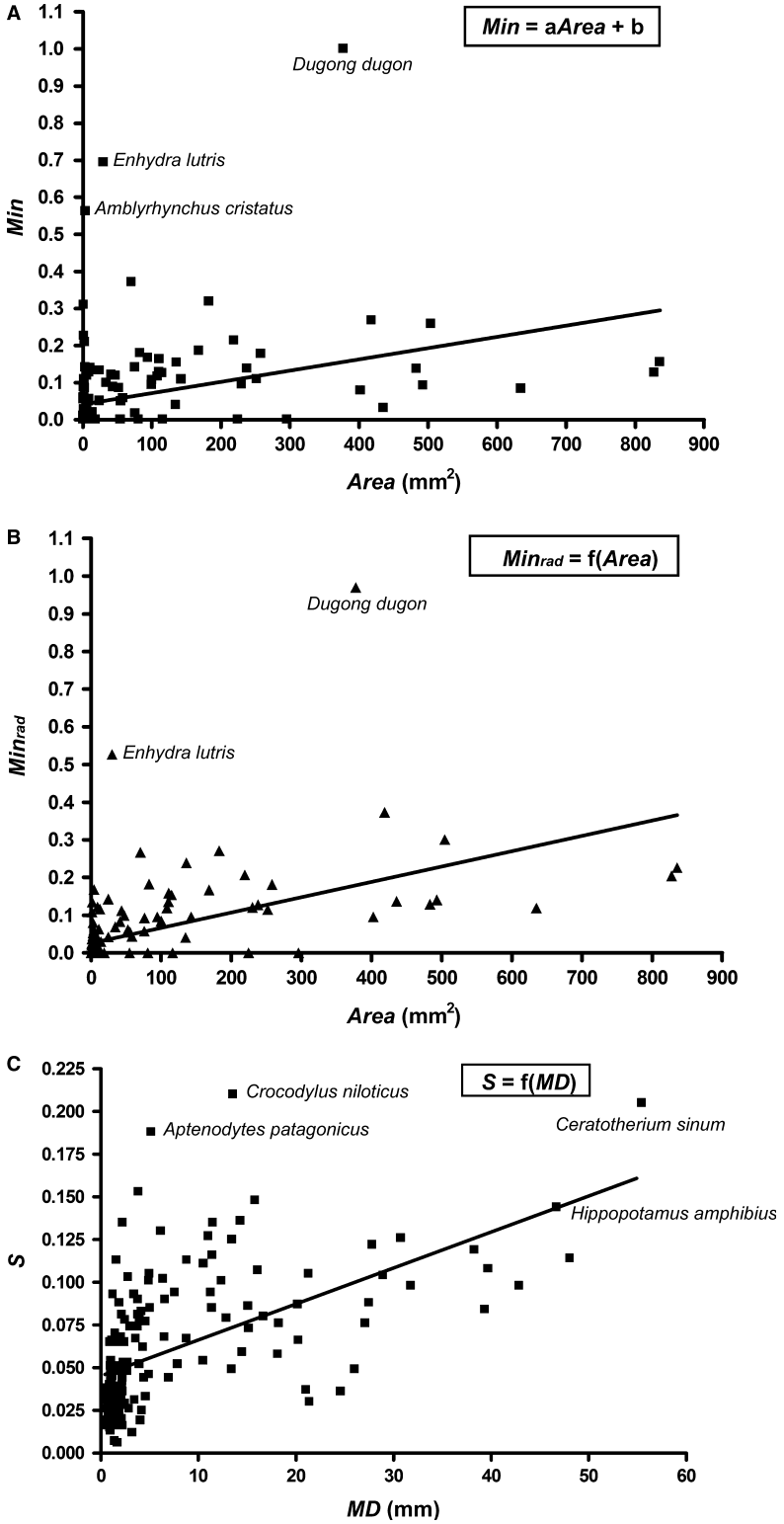

Figure 11. Linear regressions of the relationships between: *Area* (considered here as a proxy of size) and *Min* (A); *Area* and Min_{rad} (B); and *MD* and *S* (C). The variable representing size was selected to maximize significance (minimize probability; see Table 3) of the relationship. The slopes of the regression lines are all significantly different from zero ($P < 0.0001$). Regression parameters are given in Table 4.

Table 4. Parameters of the linear regressions of the relationships between (A) *Area* (considered here as a proxy of size) and *Min*; (B) *Area* and Min_{rad}; and (C) *MD* and *S*

Regression	Slope, mean ± SD	Elevation, mean ± SD	r^2
$Min = aArea + b$	$0.0003033 \pm 6.424 \times 10^5$	0.04136 ± 0.009938	0.1223
$Min_{rad} = f(Area)$	$0.0004054 \pm 5.091 \times 10^5$	0.02613 ± 0.007876	0.2839
$S = f(MD)$	$0.002109 \pm 2.467 \times 10^4$	0.04516 ± 0.003226	0.3136

For all regressions, the slope of the line displays a highly significant difference from zero ($P < 0.0001$).

which they are thought to have evolved. Hence, the nodal values inferred for lifestyle by FIC must be unreliable, which would explain the lack of power of the method, in this case. Conversely, the FIC sign test appears to be more powerful with quantitative data, which is in line with our expectations.

Concluding remarks

The present work is the first quantitative study of the microanatomical diversity of ribs in amniotes. It is complementary to previous work conducted on long bones and vertebrae because it further documents bone inner architectural diversity and offers a better understanding of the general adaptation of the skeleton to environmental and biomechanical constraints. From all the studies carried out on the diversity of bone microanatomy in tetrapods, it appears that the appendicular skeleton bears a stronger ecological signal than the axial skeleton. Lifestyle is one of the main factors explaining limb bone compactness. Although an ecological signal has been detected in vertebral and rib inner structures, body size appears to be a major structural constraint in the axial skeleton.

The relationship between lifestyle and rib microanatomy remains to be further documented and understood. We considered only a specific region of the rib series for our analyses. The patterns of intraspecific microanatomical variability in the rib series and within a single element have received little attention. Nevertheless, the rib or the rib level cannot always be selected in palaeoecological studies because the fossil record is often fragmentary, and not all fossil material can be sectioned. For palaeobiological application of the present findings, it would be important to test whether the relationship found in the present study still holds true when another rib or another section of the rib is considered.

ACKNOWLEDGEMENTS

We thank all of the individuals and institutions who have lent or given specimens for the present study: Didier Berthet (musée des Confluences, Centre de Conservation et d'Étude des Collections, Lyon, France); Eileen Westwig (American Museum of Natural History, New York, NY, USA); Christine Lefevre and Salvador Bailon (Muséum National d'Histoire Naturelle, Paris, France); and Wolfgang Böhme, Stefanie Rick, Till Töpfer, Rainer Hutterer and Jan Decher (Zoological Research Museum Alexander Koenig, Bonn, Germany). We thank Eli Amson and Alexandra Houssaye for their helpful comments and suggestions that improved the manuscript. We are also grateful to the editor, John A. Allen, for his efficient handling of the draft. AC acknowledges financial support received from the Alexander von Humboldt Foundation. VB and ML were financed by the recurring grants to the CR2P by the CNRS and the French Ministry of Research.

REFERENCES

Abramoff MD, Magalhães PJ, Ram SJ. 2004. Image processing with ImageJ. *Biophotonics International* **11:** 36–42.

Agnarsson I, Kuntner M, May-Collado LJ. 2010. Dogs, cats, and kin: a molecular species-level phylogeny of Carnivora. *Molecular Phylogenetics and Evolution* **54:** 726–745.

Agnarsson I, Zambrana-Torrelio CM, Flores-Saldana NP, May-Collado LJ. 2011. A time-calibrated species-level phylogeny of bats (Chiroptera, Mammalia). *PLoS Currents* **3:** RRN1212.

Amson E, de Muizon C, Laurin M, Argot C, de Buffrénil V. 2014. Gradual adaptation of bone structure to aquatic lifestyle in extinct sloths from Peru. *Proceedings of the Royal Society of London Series B, Biological Sciences* **281:** 20140192.

Asher RJ, Lin KH, Kardjilov N, Hautier L. 2011. Variability and constraint in the mammalian vertebral column. *Journal of Evolutionary Biology* **24:** 1080–1090.

Benjamini Y, Hochberg Y. 1995. Controlling the false discovery rate: a practical and powerful approach to multiple testing. *Journal of the Royal Statistical Society Series B (Methodological)* **57:** 289–300.

Bibi F. 2013. A multi-calibrated mitochondrial phylogeny of extant Bovidae (Artiodactyla, Ruminantia) and the importance of the fossil record to systematics. *BMC Evolutionary Biology* **13:** 1–15.

Blankers T, Townsend TM, Pepe K, Reeder TW, Wiens JJ. 2013. Contrasting global-scale evolutionary radiations: phylogeny, diversification, and morphological evolution in the major clades of iguanian lizards. *Biological Journal of the Linnean Society* **108:** 127–143.

Bramble DM, Carrier DR. 1983. Running and breathing in mammals. *Science* **219:** 251–256.

de Buffrénil V, Francillon-Vieillot H. 2001. Ontogenetic changes in bone compactness in male and female Nile monitors (*Varanus niloticus*). *Journal of Zoology* **254:** 539–546.

de Buffrénil V, Rage JC. 1993. La "pachyostose" vertébrale de *Simoliophis* (Reptilia, Squamata): données comparatives et considérations fonctionnelles. *Annales de Paléontologie* **79:** 315–335.

de Buffrénil V, Schoevaert D. 1989. Données quantitatives et observations histologiques sur la pachyostose du squelette du dugong, *Dugong dugon* (Müller) (Sirenia, Dugongidae). *Canadian Journal of Zoology* **67:** 2107–2119.

de Buffrénil V, Sire JY, Schoevaert D. 1986. Comparaison de la structure et du volume squelettiques entre un delphinidé (*Delphinus delphis* L.) et un mammifère terrestre (*Panthera leo* L.). *Canadian Journal of Zoology* **64:** 1750–1756.

de Buffrénil V, de Ricqlès A, Ray CE, Domning DP. 1990. Bone histology of the ribs of the archaeocetes (Mammalia: Cetacea). *Journal of Vertebrate Paleontology* **10:** 455–466.

de Buffrénil V, Bardet N, Pereda-Superbiola X, Bouya B. 2008. Specialization of bone structure in *Pachyvaranus crassispondylus* Arambourg, 1952, an aquatic squamate from the Late Cretaceous of the southern Tethyan margin. *Lethaia* **41:** 59–69.

de Buffrénil V, Canoville A, D'Anastasio R, Domning DP. 2010. Evolution of sirenian pachyosteosclerosis, a model-case for the study of bone structure in aquatic tetrapods. *Journal of Mammalian Evolution* **17:** 101–120.

Canoville A, Laurin M. 2009. Microanatomical diversity of the humerus and lifestyle in lissamphibians. *Acta Zoologica* **90:** 110–122.

Canoville A, Laurin M. 2010. Evolution of humeral microanatomy and lifestyle in amniotes, and some comments on palaeobiological inferences. *Biological Journal of the Linnean Society* **100:** 384–406.

Carrier DR. 1996. Function of the intercostal muscles in trotting dogs: ventilation or locomotion? *Journal of Experimental Biology* **199:** 1455–1465.

Casha AR, Camilleri L, Manché A, Gatt R, Attard D, Gauci M, Camilleri-Podesta M-T, Grima JN. 2015a. External rib structure can be predicted using mathematical models: an anatomical study with application to understanding fractures and intercostal muscle function. *Clinical Anatomy* **28:** 512–519.

Casha AR, Camilleri L, Manché A, Gatt R, Attard D, Gauci M, Camilleri-Podesta M-T, McDonald S, Grima JN. 2015b. Internal rib structure can be predicted using mathematical models: an anatomic study comparing the chest to a shell dome with application to understanding fractures. *Clinical Anatomy* **28:** 1008–1016.

Clack JA. 2002. *Gaining ground: the origin and evolution of tetrapods*. Indiana University Press: Bloomington, IN, USA. 396 pp.

Conrad JL, Ast JC, Montanari S, Norell MA. 2011. A combined evidence phylogenetic analysis of Anguimorpha (Reptilia: Squamata). *Cladistics* **27:** 230–277.

Cooper LN, Seiffert ER, Clementz M, Madar SI, Bajpai S, Hussain ST, Thewissen JGM. 2014. Anthracobunids from the Middle Eocene of India and Pakistan are stem perissodactyls. *PLoS ONE* **9:** e109232.

Cubo J, Ponton F, Laurin M, de Margerie E, Castanet J. 2005. Phylogenetic signal in bone microstructure of sauropsids. *Systematic Biology* **54:** 562–574.

Curran-Everett D. 2000. Multiple comparisons: philosophies and illustrations. *American Journal of Physiology – Regulatory Integrative and Comparative Physiology* **279:** 1–8.

Currey JD, Alexander R. 1985. The thickness of the walls of tubular bones. *Journal of Zoology* **206:** 453–468.

D'Emic MD, Smith KM, Ansley ZT. 2015. Unusual histology and morphology of the ribs of mosasaurs (Squamata). *Palaeontology* **58:** 511–520.

Domning DP, de Buffrénil V. 1991. Hydrostasis in the Sirenia: quantitative data and functional interpretations. *Marine Mammal Science* **7:** 331–368.

Dumont M, Laurin M, Jacques F, Pellé E, Dabin W, de Buffrénil V. 2013. Inner architecture of vertebral centra in terrestrial and aquatic mammals: a two-dimensional comparative study. *Journal of Morphology* **274:** 570–584.

Eltringham SK. 1993. The pygmy hippopotamus (*Hexaprotodon liberiensis*). In: Oliver LR, ed. *Pigs, peccaries, and hippos*. Gland: IUCN, 55–60.

Felsenstein J. 1985. Phylogenies and the comparative method. *The American Naturalist* **125:** 1–15.

Fish FE. 1996. Transitions from drag-based to lift-based propulsion in mammalian swimming. *American Zoologist* **36:** 628–641.

Fish FE, Stein BR. 1991. Functional correlates of differences in bone density among terrestrial and aquatic genera in the family Mustelidae (Mammalia). *Zoomorphology* **110:** 339–345.

Fujiwara SI, Kuwazuru O, Inuzuka N, Yoshikawa N. 2009. Relationship between scapular position and structural strength of rib cage in quadruped animals. *Journal of Morphology* **270:** 1084–1094.

Galewski T, Tilak M-K, Sanchez S, Chevret P, Paradis E, Douzery EJ. 2006. The evolutionary radiation of Arvicolinae rodents (voles and lemmings): relative contribution of nuclear and mitochondrial DNA phylogenies. *BMC Evolutionary Biology* **6:** 1–17.

Germain D, Laurin M. 2005. Microanatomy of the radius and lifestyle in amniotes (Vertebrata, Tetrapoda). *Zoologica Scripta* **34:** 335–350.

Girondot M, Laurin M. 2003. Bone profiler: a tool to quantify, model, and statistically compare bone-section compactness profiles. *Journal of Vertebrate Paleontology* **23:** 458–461.

Hassanin A, Delsuc F, Ropiquet A, Hammer C, van Vuuren BJ, Matthee C, Ruiz-Garcia M, Catzeflis F,

Areskoug V, Nguyen TT, Couloux A. 2012. Pattern and timing of diversification of Cetartiodactyla (Mammalia, Laurasiatheria), as revealed by a comprehensive analysis of mitochondrial genomes. *Comptes Rendus Biologies* **335:** 32–50.

Hayashi S, Houssaye A, Nakajima Y, Chiba K, Ando T, Sawamura H, Inusuka N, Kaneko N, Osaki T. 2013. Bone inner structure suggests increasing aquatic adaptations in Desmostylia (Mammalia, Afrotheria). *PLoS ONE* **8:** e59146.

Hedges SB, Vidal N. 2009. Lizards, snakes, and amphisbaenians (Squamata). In: Hedges SB, Kumar S, eds. *The timetree of life*. Oxford: Oxford University Press, 383–389.

Heide-Jørgensen MP, Richard PR, Rosing-Asvid A. 1998. Dive patterns of belugas (*Delphinapterus leucas*) in waters near Eastern Devon Island. *Arctic* **51:** 17–26.

Heinrich JT. 2015. Spatial characterization of rib cortical bone microstructure and the effect of nutritional and physiological stresses. PhD Thesis, University of Toronto.

Houssaye A. 2009. 'Pachyostosis' in aquatic amniotes: a review. *Integrative Zoology* **4:** 325–340.

Houssaye A. 2013. Palaeoecological and morphofunctional interpretation of bone mass increase: an example in Late Cretaceous shallow marine squamates. *Biological Reviews* **88:** 117–139.

Houssaye A, Bardet N. 2012. Rib and vertebral micro-anatomical characteristics of hydropelvic mosasauroids. *Lethaia* **45:** 200–209.

Houssaye A, Mazurier A, Herrel A, Volpato V, Tafforeau P, Boistel R, de Buffrénil V. 2010. Vertebral microanatomy in squamates: structure, growth and ecological correlates. *Journal of Anatomy* **217:** 715–727.

Houssaye A, Boistel R, Böhme W, Herrel A. 2013. Jack-of-all-trades master of all? Snake vertebrae have a generalist inner organization. *Naturwissenschaften* **100:** 997–1006.

Houssaye A, Tafforeau P, Herrel A. 2014. Amniote vertebral microanatomy – what are the major trends? *Biological Journal of the Linnean Society* **112:** 735–746.

Houssaye A, Tafforeau P, de Muizon C, Gingerich PD. 2015a. Transition of Eocene whales from land to sea: evidence from bone microstructure. *PLoS ONE* **10:** e0118409.

Houssaye A, Waskow A, Hayashi S, Cornette R, Lee AH, Hutchinson JR. 2015b. Biomechanical evolution of solid bones in large animals: a microanatomical investigation. *Biological Journal of the Linnean Society* **117:** 350–371.

Ibrahim N, Sereno PC, Dal Sasso C, Maganuco S, Fabbri M, Martill DM, Zouhri S, Myhrvold N, Iurino DA. 2014. Semiaquatic adaptations in a giant predatory dinosaur. *Science* **345:** 1613–1616.

IUCN 2015. The IUCN Red List of Threatened Species, Version 2015-3. Accessed at http://www.iucnredlist.org.

Jarvis ED, Mirarab S, Aberer AJ, Li B, Houde P, Li C, Ho SWY, Faircloth BC, Nabholz B, Howard JT, Suh A, Weber CC, da Fonseca RR, Li J, Zhang F, Li H, Zhou L, Narula N, Liu L, Ganapathy G, Boussau B, Bayzid MS, Zavidovych V, Subramanian S, Gabaldón T, Capella-Gutiérrez S, Huerta-Cepas J, Rekepalli B, Munch K, Schierup M, Lindow B, Warren WC, Ray D, Green RE, Bruford MW, Zhan X, Dixon A, Li S, Li N, Huang Y, Derryberry EP, Bertelsen MF, Sheldon FH, Brumfield RT, Mello CV, Lovell PV, Wirthlin M, Cruz Schneider MP, Prosdocimi F, Samaniego JA, Vargas Velazquez AM, Alfaro-Núñez A, Campos PF, Petersen B, Sicheritz-Ponten T, Pas A, Bailey T, Scofield P, Bunce M, Lambert DM, Zhou Q, Perelman P, Driskell AC, Shapiro B, Xiong Z, Zeng Y, Liu S, Li Z, Liu B, Wu K, Xiao J, Yinqi X, Zheng Q, Zhang Y, Yang H, Wang J, Smeds L, Rheindt FE, Braun M, Fjeldsa J, Orlando L, Barker FK, Jønsson KA, Johnson W, Koepfli KPO, Brien S, Haussler D, Ryder OA, Rahbek C, Willerslev E, Graves GR, Glenn TC, McCormack J, Burt D, Ellegren H, Alström P, Edwards SV, Stamatakis A, Mindell DP, Cracraft J, Braun EL, Warnow T, Jun W, Gilbert MTP, Zhang G. 2014. Whole-genome analyses resolve early branches in the tree of life of modern birds. *Science* **346:** 1320–1331.

Jenkins FA Jr. 1970. Anatomy and function of expanded ribs in certain edentates and primates. *Journal of Mammalogy* **51:** 288–301.

Josse S, Moreau T, Laurin M. 2006. Stratigraphic tools for Mesquite. Available at: http://mesquiteproject.org/packages/stratigraphicTools.

Konietzko-Meier D, Danto M, Gądek K. 2014. The microstructural variability of the intercentra among temnospondyl amphibians. *Biological Journal of the Linnean Society* **112:** 747–764.

Kriloff A, Germain D, Canoville A, Vincent P, Sache M, Laurin M. 2008. Evolution of bone microanatomy of the tetrapod tibia and its use in palaeobiological inference. *Journal of Evolutionary Biology* **21:** 807–826.

Kumar S, Hedges SB. 2011. TimeTree2: species divergence times on the iPhone. *Bioinformatics* **27:** 2023–2024.

Lamm ET. 2013. Preparation and sectioning of specimens. In: Padian K, Lamm ET, eds. *Bone histology of fossil tetrapods: advancing methods, analysis, and interpretation*. Berkeley, CA: University of California Press, 55–160.

Laurin M. 2004. The evolution of body size, Cope's rule and the origin of amniotes. *Systematic Biology* **53:** 594–622.

Laurin M, Girondot M, Loth MM. 2004. The evolution of long bone microstructure and lifestyle in lissamphibians. *Paleobiology* **30:** 589–613.

Laurin M, Canoville A, Germain D. 2011. Bone microanatomy and lifestyle: a descriptive approach. *Comptes Rendus Palevol* **10:** 381–402.

Li Z, Kindig MW, Subit D, Kent RW. 2010. Influence of mesh density, cortical thickness and material properties on human rib fracture prediction. *Medical Engineering & Physics* **32:** 998–1008.

Luiselli L, Akani GC, Capizzi D. 1999. Is there any interspecific competition between dwarf crocodiles (*Osteolaemus tetraspis*) and Nile monitors (*Varanus niloticus ornatus*) in the swamps of central Africa? A study from South-Eastern Nigeria. *Journal of Zoology* **247:** 127–131.

Lyson TR, Bever GS, Scheyer TM, Hsiang AY, Gauthier JA. 2013. Evolutionary origin of the turtle shell. *Current Biology* **23:** 1113–1119.

Maddison WP. 1991. Squared-change parsimony reconstructions of ancestral states for continuous-valued characters on a phylogenetic tree. *Systematic Zoology* **40:** 304–314.

Maddison WP. 2000. Testing character correlation using pairwise comparisons on a phylogeny. *Journal of Theoretical Biology* **202:** 195–204.

Maddison WP, Maddison DR. 2014. Mesquite: a modular system for evolutionary analysis, Version 3. Available at: http://mesquiteproject.org

de Margerie E, Sanchez S, Cubo J, Castanet J. 2005. Torsional resistance as a principal component of the structural design of long bones: comparative multivariate evidence in birds. *The Anatomical Record* **282:** 49–66.

Martin AR, Silva VD. 2004. River dolphins and flooded forest: seasonal habitat use and sexual segregation of botos (*Inia geoffrensis*) in an extreme cetacean environment. *Journal of Zoology* **263:** 295–305.

Meier PS, Bickelmann C, Scheyer TM, Koyabu D, Sánchez-Villagra MR. 2013. Evolution of bone compactness in extant and extinct moles (Talpidae): exploring humeral microstructure in small fossorial mammals. *BMC Evolutionary Biology* **13:** 55.

Meredith RW, Janečka JE, Gatesy J, Ryder OA, Fisher CA, Teeling EC, Goodbla A, Eizirik E, Simão TLL, Stadler T, Rabosky DL, Honeycutt RL, Flynn JJ, Ingram CM, Steiner C, Williams TL, Robinson TJ, Burk-Herrick A, Westerman M, Ayoub NA, Springer MS, Murphy WJ. 2011. Impacts of the Cretaceous terrestrial revolution and KPg extinction on mammal diversification. *Science* **334:** 521–524.

Midford P, Garland TJ, Maddison WP. 2010. Pdap Package for Mesquite. Available at: http://mesquiteproject.org/pdap_mesquite/index.html

Mitton D, Minonzio JG, Talmant M, Ellouz R, Rongieras F, Laugier P, Bruyère-Garnier K. 2014. Nondestructive assessment of human ribs mechanical properties using quantitative ultrasound. *Journal of Biomechanics* **47:** 1548–1553.

Mosauer W. 1932. On the locomotion of snakes. *Science* **76:** 583–585.

Myers P, Espinosa R, Parr CS, Jones T, Hammond GS, Dewey TA. 2015. The Animal Diversity Web (online). Accessed at http://animaldiversity.org.

Nakajima Y, Hirayama R, Endo H. 2014. Turtle humeral microanatomy and its relationship to lifestyle. *Biological Journal of the Linnean Society* **112:** 719–734.

Oaks JR. 2011. A time-calibrated species tree of Crocodylia reveals a recent radiation of the true crocodiles. *Evolution* **65:** 3285–3297.

Pierce SE, Ahlberg PE, Hutchinson JR, Molnar JL, Sanchez S, Tafforeau P, Clack JA. 2013. Vertebral architecture in the earliest stem tetrapods. *Nature* **494:** 226–229.

Pyron RA, Burbrink FT, Wiens JJ. 2013. A phylogeny and revised classification of Squamata, including 4161 species of lizards and snakes. *BMC Evolutionary Biology* **13:** 93.

Quémeneur S, de Buffrénil V, Laurin M. 2013. Microanatomy of the amniote femur and inference of lifestyle in limbed vertebrates. *Biological Journal of the Linnean Society* **109:** 644–655.

Reynolds RG, Niemiller ML, Revell LJ. 2014. Toward a Tree-of-Life for the boas and pythons: Multilocus species-level phylogeny with unprecedented taxon sampling. *Molecular Phylogenetics and Evolution* **71:** 201–213.

de Ricqlès A, de Buffrénil V. 2001. Bone histology, heterochronies and the return of tetrapods to life in water: w[h]ere are we? In: Mazin JM, de Buffrénil V, eds. *Secondary Adaptation of Tetrapods to Life in Water*. Munich: Dr Friedrich Pfeil, 289–310.

Scheyer TM, Sander PM. 2007. Shell bone histology indicates terrestrial palaeoecology of basal turtles. *Proceedings of the Royal Society of London Series B, Biological Sciences* **274:** 1885–1893.

Swartz SM, Parker A, Huo C. 1998. Theoretical and empirical scaling patterns and topological homology in bone trabeculae. *The Journal of Experimental Biology* **201:** 573–590.

Taylor MA. 2000. Functional significance of bone ballastin in the evolution of buoyancy control strategies by aquatic tetrapods. *Historical Biology* **14:** 15–31.

Teeling E. 2009. Bats (Chiroptera). In: Hedges SB, Kumar S, eds. *The timetree of life*. New York, NY: Oxford University Press, 499–503.

Tickle PG, Ennos AR, Lennox LE, Perry SF, Codd JR. 2007. Functional significance of the uncinate processes in birds. *Journal of Experimental Biology* **210:** 3955–3961.

Townsend TM, Mulcahy DG, Noonan BP, Sites JW Jr, Kuczynski CA, Wiens JJ, Reeder TW. 2011. Phylogeny of iguanian lizards inferred from 29 nuclear loci, and a comparison of concatenated and species-tree approaches for an ancient, rapid radiation. *Molecular Phylogenetics and Evolution* **61:** 363–380.

Vidal N, Rage J-C, Couloux A, Hedges SB. 2009. Snakes (Serpentes). In: Hedges SB, Kumar S, eds. *The timetree of life*. Oxford: Oxford University Press, 390–397.

Wake DB. 1979. The endoskeleton: the comparative anatomy of the vertebral column and ribs. In: Wake MH, ed. *Hyman's comparative vertebrate anatomy*. Chicago, IL: The University of Chicago Press, 192–237.

Wall WP. 1983. The correlation between high limb-bone density and aquatic habits in recent mammals. *Journal of Paleontology* **57:** 197–207.

Waskow K, Sander PM. 2014. Growth record and histological variation in the dorsal ribs of *Camarasaurus* sp. (Sauropoda). *Journal of Vertebrate Paleontology* **34:** 852–869.

Webb PW, de Buffrénil V. 1990. Locomotion in the biology of large aquatic tetrapods. *Transactions of the American Fisheries Society* **119:** 629–641.

Wiens JJ, Lambert SM. 2014. The phylogeny of lizard families. In Rheubert JL, Siegel DS, Trauth SE, eds. *Reproductive biology and phylogeny of Lizards and Tuatara*. Boca Raton, FL: CRC Press, 27–42.

Wiens JJ, Hutter CR, Mulcahy DG, Noonan BP, Townsend TM, Sites JW, Reeder TW. 2012. Resolving the phylogeny of lizards and snakes (Squamata) with extensive sampling of genes and species. *Biology Letters* **8:** 1043–1046.

Yoganandan N, Pintar FA. 1998. Biomechanics of human thoracic ribs. *Journal of Biomechanical Engineering* **120:** 100–104.

Yonezawa T, Nikaido M, Kohno N, Fukumoto Y, Okada N, Hasegawa M. 2007. Molecular phylogenetic study on the origin and evolution of Mustelidae. *Gene* **396:** 1–12.

SUPPORTING INFORMATION

Additional Supporting Information may be found online in the supporting information tab for this article:

Table S1. Dataset compiled in the present study, and containing the list of species sampled, the scores of lifestyle according to two coding schemes (our initial, 10-state coding, and the coding with eight states used for the statistical analyses), the size parameters measured for each species, and the compactness profile parameters obtained in BONE PROFILER (Girondot & Laurin, 2003).